Maximizing the Secrecy Energy Efficiency of the Cooperative Rate-Splitting Aided Downlink in Multi-Carrier UAV Networks

Hamed Bastami, Majid Moradikia, Ahmed Abdelhadi, *Senior Member, IEEE,* Hamid Behroozi, *Member, IEEE,* Bruno Clerckx, *Fellow, IEEE,* and Lajos Hanzo, *Life Fellow, IEEE* .

***Abstract*—Although Unmanned Aerial Vehicles (UAVs) are capable of significantly improving the information security by detecting the eavesdropper's location, their limited energy motivates our research to propose a secure and energy efficient scheme. Thanks to the common-message philosophy introduced by Rate-Splitting (RS), we no longer have to allocate a portion of the transmit power to radiate Artificial Noise (AN), and yet both the Energy Efficiency (EE) and secrecy can be improved. Hence we define and study the Secrecy Energy Efficiency (SEE) of a multi-carrier multi-UAV network, in which Cooperative Rate-Splitting (CRS) is employed by each multi-antenna UAV Base-Station (UAV-BS) for protecting their downlink transmissions against an external eavesdropper (Eve). Furthermore, we consider the challenging scenario in which CRS is employed by each multi-antenna UAV-BS to protect their corresponding downlink transmissions against an external Eve. We further consider a difficult scenario in terms of security in which only imperfect channel state information of Eve is available at the Tx. Accordingly, we conceive a robust secure resource allocation algorithm, which maximizes the SEE by jointly optimizing both the user association matrix and the network parameter allocation problem, including the RS precoders, time slot sharing and power allocation. Due to the non-convexity of the problem, it is decoupled into a pair of convex sub-problems. Firstly, new two-tier intra-cell optimization problems are formulated for achieving ξ-optimal solutions by iterative block coordinate decent programming. Then, the power of each sub-channel is optimized by formulating the associated power control problem. Simulation results confirm that the scheme conceived enhances both the secrecy and energy efficiency of the system compared to the existing cooperative non-orthogonal benchmarks.**

***Index Terms*—Rate splitting, physical layer security, robust beamforming, secrecy energy efficiency, imperfect CSIT, worst-case optimization, cellular UAV networks.**

Hamed Bastami and Hamid Behroozi are with the Department of Electrical Engineering, Sharif University of Technology, Tehran, Iran, e-mails: {hamed.bastami@ee., behroozi@}sharif.edu

Majid Moradikia and Ahmed Abdelhadi are with the Engineering Technology Department at University of Houston, e-mails:{mmoradikia,aabdelhadi}@uh.edu.

Bruno Clerckx is with the Department of Electrical and Electronic Engineering, Imperial College London, London SW7 2AZ, U.K. (e-mail: b.clerckx@imperial.ac.uk).

Lajos Hanzo is with the University of Southampton, Southampton SO17 1BJ, U.K, e-mail: hanzo@soton.ac.uk.

L. Hanzo would like to acknowledge the financial support of the Engineering and Physical Sciences Research Council projects *EP/P034284/1* and *EP/P003990/1* (COALESCE) as well as of the European Research Council's Advanced Fellow Grant QuantCom (*Grant No. 789028*)

I. Introduction

GIVEN the rapid evolution of the cellular Internet-of-Things (IoT), Next Generation (NextG) systems are expected to support heterogeneous services for a massive number of users [1], [2]. In this context, both energy efficiency as well as security occupy center stage [3].

Physical layer security (PLS) is regarded as a promising design alternative to upper-layer cryptographic techniques in wireless networks. The principle of PLS is to opportunistically exploit the random characteristics of fading channels, where the legitimate link is expected to experience a better condition than that of the eavesdroppers (Eve) [4]-[10]. Among different multi-antenna techniques, beamforming and jamming have been extensively utilized as the most effective techniques for guaranteeing secure communication[1] [6]-[8]. While jamming is capable of intentionally injecting specifically designed Artificial Noise (AN) for confusing the $Eves$. As another potent design alternative, beamforming aims for focusing the information-bearing signal towards the legitimate user, while mitigating its leakage to $Eves$ by transmitting over the null-space of the spatial channels spanned by the $Eves$. Although several authors considered the problem of secrecy rate maximization [6], for striking a tradeoff between the secrecy rate and the energy consumption, maximizing the secrecy energy efficiency (SEE) as the objective function is preferred [14]-[17]. Notably, both the performance and the design of the aforementioned PLS schemes significantly depends on the accuracy of the knowledge about the Eve's channel state information at the transmitter (E-CSIT) [9], [18], [19].

Recently, thanks to the high mobility, on-demand coverage, and to the availability of the line-of-sight (LoS) link, unmanned aerial vehicle (UAV) aided communications have attracted significant research interests [15], [19]-[23]. In particular, with the aim of mitigating the traffic load imposed on the terrestrial BS, UAVs can be harnessed as aerial-BSs [20]. Furthermore, the PLS can be readily improved by UAVs upon detecting the Eve's location via the UAV-mounted cameras or radar [15][2][3]. Explicitly, only imperfect E-CSIT may be

[1]To implement the above-mentioned PLS techniques several solutions have been proposed in the literature [11], [12], [13].

[2]There are several PLS studies that adopted their strategy based on the Eve's direction knowledge [20], [21], e.g., at airports, in which the $Eves$ might be UAVs as well [22].

[3]By deploying either a camera or two radios including one for transmission-reception and one for the radar, there is no need for the monitoring mode to acquire the Eve's CSI by imposing an additional overhead.

TABLE I
OVERVIEW OF EXISTING LITERATURE

References⇒ / Keywords⇓	**Proposed Approach**	[6]	[7]	[8]	[9]	[15]	[16]	[17]	[18]	[19]	[20]	[23]	[24]	[25]	[34]	[37]	[38]	[39]
PLS	✓	✓	✓	✓	✓	✓	✓	✓	✓	✓		✓			✓		✓	✓
Beamformer (Precoder) Design	✓	✓	✓	✓	✓		✓		✓	✓	✓		✓	✓	✓	✓		
AN Design	✓	✓	✓	✓				✓		✓								✓
UAV Trajectory Design						✓						✓						
Power Allocation						✓				✓	✓					✓		✓
Unknown Eve		✓										✓						
Known Eve with Imperfect E-CSIT	✓				✓				✓	✓		✓						
UAV Communication	✓				✓	✓		✓			✓	✓	✓					
UAV-BS	✓				✓			✓			✓							
Multi-Carrier User Association	✓									✓	✓					✓		
HetNet	✓				✓						✓					✓		
RS	✓				✓				✓				✓	✓	✓			
CRS	✓														✓			
NOMA										✓	✓					✓	✓	
Worst-Case Secrecy Rate Maximization		✓			✓				✓			✓						
Secrecy Rate constraint (or Maximization)			✓	✓													✓	
SEE Maximization	✓					✓	✓	✓										✓
MISO-BC	✓				✓				✓		✓		✓	✓	✓			
Secrecy Sum-Rate Maximization															✓			
Secrecy-Based Resource Allocation	✓																	
SEE maximization of CRS-aided UAV-HetNet	✓																	

available and thus the conventional PLS schemes no longer perform at their best[4]. The most grave challenge arises from the limited energy supply of UAVs [15], [20]. Some of the associated challenges have been addressed by the energy efficient and robust PLS solutions designed for UAV-enabled scenarios in [15], [20], [23].

To satisfy the heterogeneous and massive connectivity requirements of NextG systems, sophisticated Multi-Input-Single-Output Broadcast (MISO-BC) solutions have been designed in [18], [19], [20], [24]-[34]. In this context, the recent technique of rate-splitting (RS) constitutes a promising solution capable of improving both the Energy Efficiency (EE) [25]-[30] and security [34] of wireless communications. Explicitly, a common message is introduced at source, which plays the dual role of being a desired message as well as playing the role of the AN harnessed for contaminating the Eve's link, without the need for allocating a precious portion of the transmit power to the AN [19]. As a further development, Cooperative Rate Splitting (CRS) has been investigated in [26], [33], [34], where the user having higher power is requested to opportunistically forward the decoded common message to the other user, which leads to significant secrecy rate improvement. Although RS has been reported to improve the security in [19], [34] and the EE in [25], as well as the robustness against imperfect CSIT in [35], these single-metric benefits have been reported separately. By contrast, the joint robust design striking a tradeoff between secrecy and energy efficiency in a CRS-aided UAV network has not been studied yet. As a special form of RSMA, secure non-orthogonal multiple access (NOMA) has also been proposed in [38]. However, the superimposed non-orthogonal streams are considered as "useless" in terms of secrecy, since they can be perfectly eliminated through SIC at Eve. However, the Eve can decode some superimposed streams and intercept the rest subject to reduced interference. By contrast, using RSMA, the common message will play the dual roles of the desired message as well as the artificial noise (AN) harnessed for confusing the potential Eve without the need for allocating extra transmit power to the AN.

In Heterogeneous Networks (HetNet), the small cells are typically covered by oversailing macro-cells for improving the outage probability of high-velocity users. In this context, user association is crucial for improving both the EE and spectral

[4]Although this is more realistic to consider a completely unknown Eve, who hide himself against Alice, by using UAV we can detect the Eve's location and thus having a knowledge about the $Eves$ (even imperfect E-CSIT) is reasonable. This is also valid for cases in which $Eves$ is one of the network's nodes, but unauthorized to receive the services, although even for a passive Eve, due to the inadvertently leakage of oscillator power, Eve's CSI might be estimated.

TABLE II
TABLE OF ACRONYMS

variable	Description	variable	Description
CCU	Cell-Center User	PCP	Power Control Problem
CEU	Cell-Edge User	MU	Macro User
AN	Artificial Noise	SPCA	Sequential Parametric Convex Approximation
PLS	Physical Layer Security	SIC	Successive Interference Cancellation
SEE	Secrecy Energy Efficiency	TPC	Transmit Precoder
E-CSIT	Eve's channel state information at the transmitter	A2G	Aerial to Ground
MISO-BC	Multi-Input Single-Output Broadcast Channel	DL	Downlink
CRS	Cooperative Rate Splitting	ASR	Achievable Secrecy Rate
UAV	Unmanned Areal Vehicle	ACC	Achievable Channel Capacity
HetNet	Heterogeneous Networks	EAIR	Estimated Achievable Information Rate
EE	Energy Efficiency	SINR	Signal to Interference plus Noise Ratio
CCI	Co-Channel Interference	C-NOMA	Cooperative Non-Orthogonal Multiple Access
NPAP	Network Parameter Allocation Problem	C-BF	Cooperative Beamforming
ICOP	Intra-Cell Optimization Problem	C-SDMA	Cooperative Space Division Multiple Access

efficiency. Although, many researchers have studied the joint problem of power allocation and user association for improving the EE [36], [37], only very few recent contributions have considered the radical objective of SEE optimization [38], [39]. Finally, SEE optimization relying on imperfect E-CSIT in RS networks has not been studied at all.

Given the knowledge gaps mentioned above, we consider a UAV-aided HetNet (UAV-HetNet) including an over-sailing macro BS and several UAV-aided cells as well as Macro-cell Users (MUs). The Frequency Division (FD) principle is used for sharing the spectrum available for Downlink (DL) transmission to a pair of legitimate UAV-user. Several MUs may interfere with the UAVs' communications and an Eve engages in covert wiretapping. We consider a challenging secrecy scenario in which Eve relies on powerful hardware for perfectly estimating its corresponding channels, while considering imperfect E-CSIT at the Tx. For each UAV-cell, the UAV-Tx relies on RS for concurrently communicating with both legitimate users on the same FD sub-channel (SC). Against this background, our contributions can be summarized as follows:

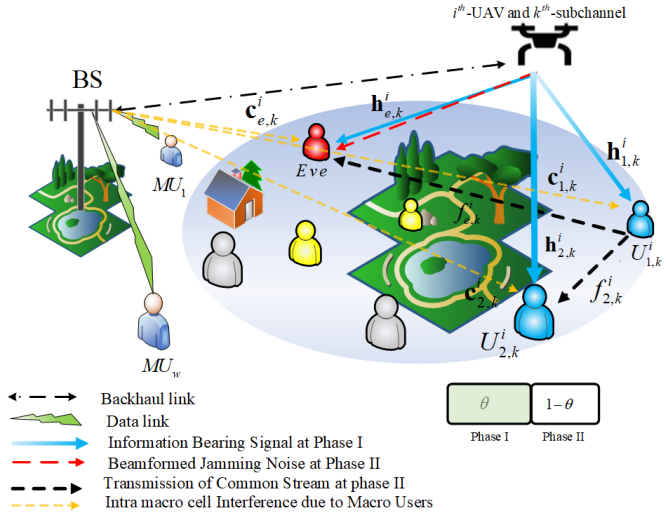

Fig. 1. Proposed system model

- This is the first treatise that considered the problem of SEE optimization under imperfect E-CSIT in RS-aided UAV networks. To cope with the security threats and with the power constraints imposed on our multi-carrier UAV-HetNet, we propose an EE-CRS-based secrecy framework, which is robust against imperfect E-CSIT and simultaneously strikes a compelling tradeoff between the secrecy rate and the energy consumption. To reach this ambitious goal, we maximize the SEE of the network considered by jointly optimizing the user association and cell parameters. As a benefit of RS, we no longer have to allocate a valuable portion of transmit power to generate AN, thus attaining both EE and secrecy.
- To exploit the benefits of CRS, each transmission slot is split into two consecutive phases. To safeguard the broadcasting phase, the RS-precoders are optimized, whilst for maintaining the security of the consecutive relaying phase, a robust beamformer is deployed at the UAV-Tx for radiating AN towards the Eve. To take full advantage of the CRS, we further optimize both the relaying and jamming powers, as well as the time slot sharing ratio between the pair of cooperative phases, leading to further boosted SEE. Additionally, as the macro-cell is assumed to have higher priority in using the spectrum available, the Co-Channel Interference (CCI) imposed on MUs by UAV communications must be controlled for maximizing the SEE.
- To satisfy the ambitious objectives of 6G, we consider a comprehensive system model, where we concurrently deploy UAV-BS (to support massive connectivity and ubiquitous access), novel energy efficient MA techniques (to support massive connectivity as well as energy efficiency while efficiently using the available resources), as well as an energy efficient multi-carrier deployment (to satisfy the massive connectivity as well as energy efficiency re-

TABLE III
TABLE OF MATH VARIABLES

Channel from UAV_i to n-th legitimate user/Eve through k-th SC	$\mathbf{h}_{n,k}^i$, $n \in \{1,2,e\}$
Channel from CCU to CEU/Eve through k-th Sc	$f_{n,k}^i$, $n \in \{2,e\}$
n-th legitimate user at i-th UAV cell through k-th SC	$U_{n,k}^i$
Transmit precoder of private streams for $U_{n,k}^i$	$\mathbf{p}_{n,k}^{i,p}$
Transmit precoder of common streams	$\mathbf{p}_k^{i,c}$
Time-slot allocation parameter	θ
Received SINR values of common stream for $U_{n,k}^i$ during the j-th phase	$\gamma_{n,k}^{i,\mathrm{c}\ (j)}$
Received SINR values of private stream of $U_{n,k}^i$ during the first phase	$\gamma_{n,k}^{i,\mathrm{p}\ (1)}$
Estimated SINR of Eve for detecting the private streams of $U_{n,k}^i$during the j-th phase	$\hat{\gamma}_{e,k}^{i,c^{(j)}}$
Commom capacity achieved by the legitimate users/Eve during the j-th phase	$C_{n,k}^{i,c\ (j)}$
Private capacity achieved by the legitimate users/Eve during the j-th phase	$C_{n,k}^{i,p\ (j)}$
SEE achieved through the k-th SC for the i-th UAV cell	$\eta_{SEE_k^i}$

quirement while efficiently using the available resources). We have to mention that the construction of the proposed secure and energy efficient multi-carrier RSMA is quite challenging, because the user-association matrix of the multi-carrier assignment as well as the power control determining the power allocated to the common sub-channels of various UAV-cells impose strong dependence among the variables of each UAV-cell.

- To deal with the resultant non-convex SEE problem we consider a decomposition approach, where a Networking Parameter Allocation Problem (NPAP) is solved, while the user association matrix is estimated. More explicitly, the NPAP is solved by the block coordinate decent technique, where the two-tier Intra-Cell Optimization Problem (ICOP) and the associated Power Control Problem (PCP) are solved successively in an iterative manner. The latter is convex and determines the power allocated to each sub-channel. By contrast, the ICOP is non-convex, hence a sub-optimal ζ-based two tier solution is proposed, where the Sequential Parametric Convex Approximation (SPCA) technique is invoked to deal with this non-convexity.
- Our simulation results validate that the proposed framework outperforms the existing cooperative non-orthogonal benchmarks in guaranteeing secure communication at a high energy efficiency. The reason for the improvement lies in the dual exploitation of the common message.

Our contributions are boldly and explicitly contrasted to the state-of-the-art at a glance in Table I.

Notation: $(.)^{\mathrm{T}}$, $(.)^*$, $(.)^{\mathrm{H}}$, and $(.)^{-1}$ denote the transpose, conjugate, conjugate transpose, and inverse of a matrix, respectively; Matrices and vectors are denoted by upper-case and lower-case Boldface letters, respectively; $\Re e(.)$ and $\Im m(.)$ respectively denotes the real and imaginary part of a complex variable; The notation $\mathrm{Vec}(\mathbf{H})$ converts the matrix $\mathbf{H}$ to a single column vector, and $\mathbf{I}_N$ denotes the $N \times N$ identity matrix. To improve the paper's readability, we have added a table of acronyms, including the abbreviations and math variables used in this paper and depicted in Tables II and III.

II. SYSTEM MODEL AND PRELIMINARIES

Our two-tier network considered is illustrated in Fig. 1, where the first tier includes a BS supporting W number of randomly distributed MUs in its corresponding macro-cell coverage. In the second tier, I low-altitude UAVs are deployed for mitigating the burden imposed on the macro BS by serving the users in need at the edge of the macro-cell. Hence, the UAVs operate independently and are connected to the BS only through a backhaul link. For the i-th UAV cell, a UAV hovering at a fixed altitude H_i aims for communicating with the users within its range. The total bandwidth of BW is optimally shared among the users. The same spectrum is used by MUs and all the other UAV cells, hence the MUs outside the i-th UAV cell may interfere with the UAV's communications [5], hence resulting in CCI. On the other hand, the MUs are assumed to have higher priority in using the spectrum and thus the CCI inflicted by the intra-UAV-cell communications must be carefully controlled. The bandwidth BW is partitioned into K SCs $SC_k|_{k=1}^K$, each of which has a bandwidth of $B_{sc} = \frac{BW}{K}$. If we let $N_k^i|_{k=1}^K$ represent the number of users assigned to SC_k in the i-th UAV cell, the maximum number of users served by UAV_i is given by $N_{\max}^i = \sum_{k=1}^K N_k^i$. Note that to take full advantage of CRS technique, a user-pair constituted by a Cell-Center User (CCU) and a Cell-Edge User (CEU) is supported within each transmission slot. For simplicity, we assume $N_k = 2$ in this paper, i.e. $N_{\max}^i = 2K$.

A. Principles of CRS

In particular, for the i-th UAV cell, the multi-antenna assisted UAV_i communicates with the pair of legitimate users $U_{1,k}^i$ and $U_{2,k}^i$, through SC_k, while an Eve (e) silently engages in covert wiretapping. Note that, $U_{1,k}^i, U_{2,k}^i$, and Eve are equipped with a single antenna, while for UAV_i $N_t \geq 2$ transmit antennas

[5]Given that UAV-BSs have much smaller transmit power than the macro-cell BS, we neglect the CCI from the other small UAV-cells.

are used. For concurrently serving a pair of users through SC_k, UAV_i utilizes the RS technique, hence the confidential messages of each legitimate user $\mathcal{W}_{n,k}^{i}\Big|_{n=1}^{2}$ are split into the common message $\mathcal{W}_{n,k}^{i,c}$, and the private message $\mathcal{W}_{n,k}^{i,p}$. The

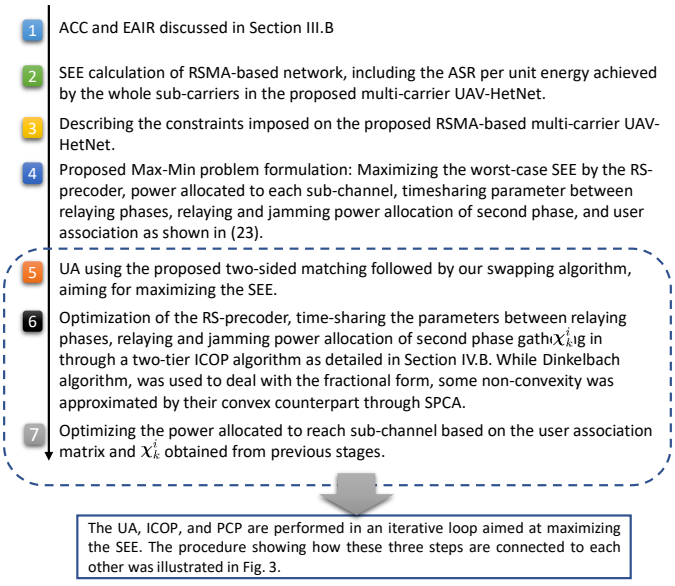

Fig. 2. Flow of mathematical analysis

so-obtained common parts $\mathcal{W}_{n,k}^{i,c}\Big|_{n=1}^{2}$ are then incorporated into a common codebook for generating the unified common stream $s_k^{i,c}$. By contrast, $\mathcal{W}_{1,k}^{i,p}$ and $\mathcal{W}_{2,k}^{i,p}$ are independently encoded into the private streams $s_{1,k}^{i,p}$, $s_{2,k}^{i,p}$, respectively. If we define $\mathbf{s}_k^i \triangleq \left[s_k^{i,c}, s_{1,k}^{i,p}, s_{2,k}^{i,p}\right]^T$ with a normalized power of $\mathbb{E}\left\{\mathbf{s}_k^i \mathbf{s}_k^{i^H}\right\} = \mathbf{I}_3$ and $\mathbf{P}_k^i \triangleq \left[\mathbf{p}_k^{i,c}, \mathbf{p}_{1,k}^{i,p}, \mathbf{p}_{2,k}^{i,p}\right] \in \mathbb{C}^{N_t \times 3}$ as the transmit precoder (TPC) matrix adopted by UAV_i, where $\mathbf{p}_k^{i,c}$, $\mathbf{p}_{1,k}^{i,p}$, and $\mathbf{p}_{2,k}^{i,p}$ respectively stand for the parts corresponding to the common and private streams, then the transmitted DL RS signal is given by:

$$\mathbf{x}_k^i = \mathbf{P}_k^i \mathbf{s}_k^i = \mathbf{p}_k^{i,c} s_k^{i,c} + \sum_{n=1}^{2} \mathbf{p}_{n,k}^{i,p} s_{n,k}^{i,p}. \tag{1}$$

We assume furthermore that the channel condition of the CCU $U_{1,k}^i$ is superior to that of the CEU $U_{2,k}^i$. Therefore, following the principle of CRS [26] at the receiver side each user first recovers $\mathcal{W}_{n,k}^{i,c}$ from the detected $s_k^{i,c}$ and then removes the common stream by performing Successive Interference Cancellation (SIC). Then, each user detects its corresponding private stream. By combining $\mathcal{W}_{n,k}^{i,c}$ at the earlier stage with the respective private message, the users capable of retrieving their original intended message $\mathcal{W}_{n,k}^{i}\Big|_{n=1}^{2}$. In the following, with the goal of helping the CEU, the CCU acts as a Decode-and-Forward (DF) cooperative node that forwards the decoded common stream to $U_{2,k}^i$. Given the half-duplex constraint, data transmission takes place in two consecutive time-slots. Hence, a dynamic time-slot allocation parameter $0 \leq \theta \leq 1$ is introduced for ensuring that the θ portion of each time slot is assigned for the broadcast phase ($UAV_i \longrightarrow \left\{U_{1,k}^i, U_{2,k}^i, e\right\}$), while the relaying phase ($U_{1,k}^i \longrightarrow \left\{U_{2,k}^i, e\right\}$) is allocated the remaining $(1-\theta)$ portion (See Fig.1). Thus, two opportunities are provided for Eve to infer the private information during these two phases of transmissions. To safeguard the first phase, the corresponding common TPC $\mathbf{p}_k^{i,c}$ is designed for ensuring that $s_k^{i,c}$ is simultaneously exploited as jamming noise for confusing Eve. By contrast, in order to secure the transmission against Eve during the relaying phase, UAV_i that is idle during this phase, serves as a friendly jammer.

B. Channel Definitions

The channel coefficients of the $UAV_i \longrightarrow \left\{U_{1,k}^i, U_{2,k}^i, e\right\}$ links spanning from the UAV to terrestrial nodes are denoted by $\mathbf{h}_{n,k}^i \in \mathbb{C}^{N_t \times 1}$ for $n \in \{1, 2, e\}$, respectively. These channels are modeled as $\mathbf{h}_{n,k}^i = d_{n,i}^{-\alpha_{n,k}^i/2} \mathbf{n}_{n,k}^i$, where $d_{n,i}^{-\alpha_{n,k}^i/2}$ represents the large scale fading characterized by the aerial to ground (A2G) distance $d_{n,i}$, and $\mathbf{n}_{n,k}^i$ $\mathcal{CN}(0, \mathbf{I})$ represents the corresponding small scale fading[67]. The path-loss exponent $\alpha_{n,k}^i$ obeys the probabilistic model of [14], which is appropriate for low-altitude UAVs comprised of both the LoS and non-LoS components $\mathcal{L}_{n,k}^i$ and $\mathcal{N}_{n,k}^i$, respectively, given by:

$$\alpha_{n,k}^i \triangleq \frac{\mathcal{L}_{n,k}^i - \mathcal{N}_{n,k}^i}{1 + \lambda_1 e^{\lambda_2 (\phi_n^i - \lambda_1)}} + \mathcal{N}_{n,k}^i, \tag{2}$$

where $\phi_n^i = \frac{180}{\pi} \sin^{-1}\left(\frac{H_i}{d_{n,i}}\right)$ denotes the elevation angle between UAV_i and the n-th user at a A2G distance $d_{n,i}$, while λ_1 and λ_2 are determined by the wireless environment, which may be urban, dense urban, etc. [14]. Additionally, $f_{n,k}^i \sim \mathcal{CN}(0,1)$ for $n \in \{2, e\}$, denotes the corresponding $U_{1,k}^i \longrightarrow \left\{U_{2,k}^i, e\right\}$ channels, during the second phase.

Remark 1. (*Imperfect E-CSIT*): In a realistic secrecy scenario, a sophisticated Eve may be able to perfectly estimate its corresponding channels, its CSI would still be outdated at the Tx owing to signaling delays, hence resulting in imperfect E-CSIT. On the other hand, as for the A2G links, the large scale fading varies smoothly and hence it can be estimated perfectly, but imperfections contaminate the small scale fading component $\mathbf{n}_{e,k}^i$.

[6]Although the model proposed in [14] constitutes an approximated form of the probabilistic LoS model, the authors of [14] have shown that that their proposed channel model represents an accurate estimate of the A2G channels. Additionally, we note that there are no optimization variables related to the dynamics of the UAV such as height or speed of the UAV in our optimization problem, which implies that determining the type of channel has no substantial impact on the subsequent analysis.

[7]The Doppler spread directly depends on the speed at which the UAV and users travel. However, in our scenario where a rotary-wing UAV operates at a fixed altitude together with the assumption of low-speed users, the value of DS would be small, i.e, $DS \simeq 0$, leading to a long coherence time, i.e., $T_c \simeq \infty$, and thus here the slow-fading model is valid [27], [28].

Based on Remark 1, to capture the resultant channel uncertainties due to Imperfect E-CSIT, we rely on the worst-case model of [18], [19], [35], formulated as follows:

$$\begin{aligned} \mathbf{n}_{e,k}^{i} &\triangleq \hat{\mathbf{n}}_{e,k}^{i} + \boldsymbol{\Delta}\mathbf{n}_{e,k}^{i}, \\ f_{e,k}^{i} &\triangleq \hat{f}_{e,k}^{i} + \triangle f_{e,k}^{i}, \end{aligned} \tag{3}$$

where $\Theta_{\mathbf{h}_e} \triangleq \left\{ \boldsymbol{\Delta}\mathbf{n}_{e,k}^{i} \in \mathbb{C}^{N_t \times 1} : \left\| \boldsymbol{\Delta}\mathbf{n}_{e,k}^{i} \right\|^2 \leq N_t \epsilon \right\}$, $\Theta_{f_e} \triangleq \left\{ \triangle f_{e,k}^{i} : \left| \triangle f_{e,k}^{i} \right|^2 \leq \epsilon \right\}$. Furthermore $\hat{\mathbf{n}}_{e,k}^{i}$ and $\hat{f}_{e,k}^{i}$ are available at the Tx $\in \left\{ U_{1,k}^{i}, UAV_i \right\}$, and they respectively stand for the estimate of $\mathbf{n}_{e,k}^{i}$, $f_{e,k}^{i}$, while $\boldsymbol{\Delta}\mathbf{n}_{e,k}^{i}$, $\Delta f_{e,k}^{i}$ denote the corresponding channel uncertainty. Specifically, $\epsilon > 0$ denotes the size of the uncertainty region in the estimated CSI of the Eve.

III. Performance Metric and Constraints

Before proceeding, we have provided a flow-diagram in Fig. 2 to show the flow of the analysis described in the sequel. In the following, after characterizing our received signal model, we calculate the Achievable Secrecy Rate (ASR) as well as achievable channel capacities (ACC) [3], which is then used for defining the SEE metric as the criterion utilized in this treatise. We note furthermore that for the sake of considering the worst-case secrecy scenario, Eve is assumed to be able to perfectly estimate its corresponding CSI, while at the legitimate UAV-Tx, only imperfect E-CSIT is available. Given this perspective, while Eve can achieve the channel capacity, Tx is only capable of achieving the estimated information rate. Thus we first derive the channel capacities and then obtain the estimated information rates, as shown in Fig. 2[8]. Next, we present the constraints imposed, which must be taken into account in our design.

A. Received Signal Model

During the first phase, UAV_i broadcasts the RS signal $\mathbf{x}_k^i$, and the node $n \in \left\{ U_{1,k}^{i},\ U_{2,k}^{i}, e \right\}$ will receive the following signal:

$$\begin{aligned} {y_{n,k}^{i}}^{(1)} = {\mathbf{h}_{n,k}^{i}}^{H} \left(\mathbf{p}_{k}^{i,c} s_{k}^{i,c} + \mathbf{p}_{1,k}^{i,p} s_{1,k}^{i,p} + \mathbf{p}_{2,k}^{i,p} s_{2,k}^{i,p} \right) + \\ \sqrt{p_k^M} {\mathbf{c}_{n,k}^{i}}^{H} \mathbf{v}_k^i + {z_{n,k}^{i}}^{(1)},\ \forall n \in \{1,2,e\}, \end{aligned} \tag{4}$$

where ${z_{n,k}^{i}}^{(1)} \sim \mathcal{CN}\left(0, \delta^2\right)$ represents the Additive White Gaussian Noise (AWGN).$\mathbf{v}_k^i$ having the power of p_k^M represents the aggregated co-channel interference (CCI) due to the communications of N_k^M number of users occupying the same channel.

In phase II, while the relaying user $U_{1,k}^{i}$ retransmits $s_k^{i,c}$ at a power level $0 \leq p_{k,R}^{i} \leq \bar{P}_R$, using the estimated channel $\hat{\mathbf{h}}_{e,k}^{i}$, the UAV_i assigns the Tx transmit beamformer of $\hat{\mathbf{p}}_{k,z}^{i} \triangleq \frac{\hat{\mathbf{h}}_{e,k}^{i}}{\|\hat{\mathbf{h}}_{e,k}^{i}\|}$ to the jamming signal z at a power of $0 \leq p_{k,J}^{i} \leq \bar{P}_J$ directed towards Eve. Given the limited power budget of phase II, we have $0 \leq p_{k,R}^{i} + p_{k,J}^{i} \leq \bar{P}_{max}^{(2)}$, which should be optimally shared between the relaying node $U_{1,k}^{i}$ and the jammer UAV_i for further enhancing the secrecy performance. Given what we discussed above, the signals received by $U_{2,k}^{i}$ and Eve in the presence of the AWGN ${z_{n,k}^{i}}^{(2)} \sim \mathcal{CN}\left(0, \delta^2\right)$ can be expressed as:

$$\begin{aligned} {y_{n,k}^{i}}^{(2)} = \sqrt{p_{k,R}^{i}} {f_{n,k}^{i}}^{H} s_k^{i,c} + \sqrt{p_{k,J}^{i}} {\mathbf{h}_{n,k}^{i}}^{H} \hat{\mathbf{p}}_{k,z}^{i} z + \\ \sqrt{p_k^M} {\mathbf{c}_{n,k}^{i}}^{H} \mathbf{v}_k^i + {z_{n,k}^{i}}^{(2)},\ \forall n \in \{2,e\}. \end{aligned} \tag{5}$$

B. ACC and EAIR

Based on above-mentioned discussions together with considering that a persistent Eve may succeed in accessing the codebooks, all the nodes $n \in \left\{ U_{1,k}^{i},\ U_{2,k}^{i}, e \right\}$ first decode $s_k^{i,c}$, while treating the private message parts as interference. Accordingly, the received SINR values encountered in detecting $s_k^{i,c}$ during the two phases, which are denoted by ${\gamma_{n,k}^{i,c}}^{(1)}$ and ${\gamma_{n,k}^{i,c}}^{(2)}$, may be expressed as follows:

$${\gamma_{n,k}^{i,c}}^{(1)} = \frac{\left| {\mathbf{h}_{n,k}^{i}}^{H} \mathbf{p}_k^{i,c} \right|^2}{\left| {\mathbf{h}_{n,k}^{i}}^{H} \mathbf{p}_{1,k}^{i,p} \right|^2 + \left| {\mathbf{h}_{n,k}^{i}}^{H} \mathbf{p}_{2,k}^{i,p} \right|^2 + p_k^M \left\| \mathbf{c}_{n,k}^{i} \right\|^2 + \delta^2}, \tag{6}$$

$$\forall n \in \{1,2,e\},$$

$${\gamma_{n,k}^{i,c}}^{(2)} = \frac{p_{k,R}^{i} \left| f_{n,k}^{i} \right|^2}{p_{k,J}^{i} \left| {\mathbf{h}_{n,k}^{i}}^{H} \hat{\mathbf{p}}_{k,z}^{i} \right|^2 + p_k^M \left\| \mathbf{c}_{n,k}^{i} \right\|^2 + \delta^2}. \tag{7}$$

$$\forall n \in \{2,e\}$$

After removing the detected signal $s_k^{i,c}$ via SIC, both $U_{1,k}^{i}$ and $U_{2,k}^{i}$ can detect their corresponding private streams. Therefore, by considering the irrelevant private stream as interference, the received SINR of the legitimate users encountered during the detection of their corresponding private information streams are obtained as:

$${\gamma_{n,k}^{i,\mathrm{p}}}^{(1)} = \frac{\left| {\mathbf{h}_{n,k}^{i}}^{H} \mathbf{p}_{n,k}^{i,p} \right|^2}{\left| {\mathbf{h}_{n,k}^{i}}^{H} \mathbf{p}_{j,k}^{i,p} \right|^2 + p_k^M \left\| \mathbf{c}_{n,k}^{i} \right\|^2 + \delta^2},\ n \neq j,$$

$$\forall n, j \in \{1,2\}. \tag{8}$$

Upon using the RS technique, an appropriate secrecy policy is to design the common TPC for ensuring that Eve is unable to decode the common stream. By doing so, $s_k^{i,c}$ can no longer be eliminated through the preceding SIC block. We also note that there is only one chance for the Eve to decipher the private messages during the first phase. Thus, from the Eve's viewpoint, the SINR associated with the detection of the private stream of $U_{n,k}^{i}$, while treating the private steam of

[8]Note that, in case of perfect CSIT, the actual channel capacity and AIR from the Tx viewpoint are equal [31]. Naturally, in the face of channel uncertainties, the channel capacity cannot be achieved by Tx, since the channels were not correctly estimated.

Algorithm 1 The algorithmic procedure of the proposed resource allocation

Start

- ❶ One user tries to match with the SC_k that does not reject it accordance to its preference list.
- ❷ Is the number of users matched with this SC equal to N_k?
  - **Yes**: Call ICOP to choose one set with the maximum $\eta_{SEE_k^i}$, according to (28).
  - **No**: The user matched with this SC successfully!
- ❸ Are there any uses left?
  - **Yes**: Go to ❶.
  - **No**: Go to ❹
- ❹ Call PCP to optimize the power of SCs according to (29).
- ❺ Are the convergence of PCP meet?
  - **Yes**: Go to ❻.
  - **No**: Go to ❶.
- ❻ Swap between tow users which can form a swapping-block pair.
- ❼ Are there any swapping-block pair left?
  - **Yes**: Go to ❻.
  - **No**: Go to ❽.
- ❽ Obtain the result of user association and network parameters for users.

End.

the other user $U_{j,k}^i\Big|_{j\neq n}$ as interference, may be expressed as:

$$\gamma_{e,n,k}^{i,\mathrm{p}\ (1)} = \frac{\left|\mathbf{h}_{e,k}^{i\ H}\mathbf{p}_{n,k}^{i,p}\right|^2}{\left|\mathbf{h}_{e,k}^{i\ H}\mathbf{p}_{k}^{i,c}\right| + \left|\mathbf{h}_{e,k}^{i\ H}\mathbf{p}_{j,k}^{i,p}\right|^2 + p_k^M\left\|\mathbf{c}_{e,k}^i\right\|^2 + \delta^2}, \quad n\neq j, \forall n,j\in\{1,2\}. \tag{9}$$

Now, the corresponding capacity achieved by the legitimate users and Eve are respectively obtained as follows:

$$C_{n,k}^{i,c\ (1)} \triangleq \theta\log_2\left(1+\gamma_{n,k}^{i,c\ (1)}\right),\ \forall n\in\{1,2,e\} \tag{10}$$

$$C_{n,k}^{i,c\ (2)} \triangleq (1-\theta)\log_2\left(1+\gamma_{n,k}^{i,c\ (2)}\right),\ \forall n\in\{2,e\} \tag{11}$$

$$C_k^{i,c} \triangleq \min\left\{\underbrace{C_{1,k}^{i,c\ (1)}}_{C_{1,k}^{i,c}}, \underbrace{C_{2,k}^{i,c\ (1)}+C_{2,k}^{i,c\ (2)}}_{C_{2,k}^{i,c}}\right\}, \tag{12}$$

$$C_{e,k}^{i,c} \triangleq C_{e,k}^{i,c\ (1)} + C_{e,k}^{i,c\ (2)}, \tag{13}$$

$$C_{n,k}^{i,p\ (1)} = C_{n,k}^{i,p} \triangleq \theta\log_2\left(1+\gamma_{n,k}^{i,p\ (1)}\right),\ \forall n\in\{1,2\} \tag{14}$$

$$C_{e,n,k}^{i,p\ (1)} = C_{e,n,k}^{i,p} \triangleq \theta\log_2\left(1+\gamma_{e,n,k}^{i,p\ (1)}\right),\ \forall n\in\{1,2\}, \tag{15}$$

where $C_k^{i,c}$ and $C_{e,k}^{i,c}$ respectively stand for the information capacity achieved by the legitimate users and Eve in detecting $s_k^{i,c}$ during the two phases. Note that as it can be observed in (13), $C_k^{i,c}$ is limited by the achievable capacity of the worst-case user. By contrast, Eve tries to infer $s_k^{c,i}$ up to the sum-capacity of both phases, as shown in (13). Additionally, $C_{n,k}^{i,p}$ represents the information capacity achieved by each of $U_{1,k}^i$, $U_{2,k}^i$ in detecting their corresponding private streams and $C_{e,n,k}^{i,p}$ denotes the information capacity achieved by Eve while aiming for detecting the private streams of the n-th user. In order to determine the estimated SINR values corresponding to the Eve's link at the UAV-Tx, the actual channel parameter $\mathbf{h}_{e,k}^i$ in (6), (7), and (9) can be readily substituted by its estimated counterpart of $\hat{\mathbf{h}}_{e,k}^i = \mathrm{PL}_{e,k}^i\cdot\ \hat{\mathbf{n}}_{e,k}^i$, given the estimated SINR values are $\hat{\gamma}_{e,k}^{i,c^{(1)}}, \hat{\gamma}_{e,k}^{i,c^{(2)}}, \hat{\gamma}_{e,n,k}^{i,p^{(1)}}$. Then, the EAIR corresponding to Eve, (the achievable capacities from the Tx viewpoint), can be written as:

$$\hat{R}_{e,k}^{i,c^{(1)}} = \theta\log_2\left(1+\hat{\gamma}_{e,k}^{i,c^{(1)}}\right) \tag{16}$$

$$\hat{R}_{e,k}^{i,c^{(2)}} = (1-\theta)\log_2\left(1+\hat{\gamma}_{e,k}^{i,c^{(1)}}\right) \tag{17}$$

$$\hat{R}_{e,n,k}^{i,p^{(1)}} = \hat{R}_{e,n,k}^{i,p} = \theta\log_2\left(1+\hat{\gamma}_{e,n,k}^{i,p^{(1)}}\right),\ \forall n\in\{1,2\} \tag{18}$$

C. Secrecy Energy Efficiency (SEE)

The SEE quantifies the ASR per unit energy and bandwidth. The total secrecy capacity of the link between UAV_i and each legitimate user is defined as the sum of the ASR values representing both the common and private parts and it is given by:

$$C_{sec,n,k}^{i,tot} \triangleq \alpha_{n,k}^i C_{sec,k}^{i,c} + C_{sec,n,k}^{i,p},\ \forall n\in\{1,2\}, \tag{19}$$

$$C_{sec,k}^{i,c} \triangleq \alpha_{n,k}^i\left[C_k^{i,c} - C_{e,k}^{i,c}\right]^+, C_{sec,n,k}^{i,p} \triangleq \left[C_{n,k}^{i,p} - C_{e,n,k}^{i,p}\right]^+,$$

where the operation $[x]^+ \triangleq \max(0,x)$, and the weighting factors $\alpha_{n,k}^i\Big|_{n=1}^2 \in [0,1]$ corresponds the proportion[9] of the secrecy rate belonged to the n-th user, and satisfies $\alpha_{1,k}^i + \alpha_{2,k}^i = 1$.

On the other hand, the overall energy consumption (EC) originates from several components: 1) Mechanical EC (E_m) of keeping the UAV aloft, 2) Circuit EC (E_c) due to active circuit blocks, 3) Transmit power EC (E_t). Given the total energy ΔE_{tot} dissipated within Δt, the SEE achieved through the k-th SC for the i-th UAV cell is given by:

$$\eta_{SEE_k^i} \triangleq \frac{\sum_{n=1}^{2}\mathcal{U}_{n,k}^i C_{sec,n,k}^{i,tot}}{(\Delta E_{tot}/\Delta t)} = \frac{\sum_{n=1}^{2}\mathcal{U}_{n,k}^i C_{sec,n,k}^{i,tot}}{P_{tot}\left(\mathbf{P}_k^i\right)}, \tag{20}$$

where $P_{tot}\left(\mathbf{P}_k^i\right) \triangleq P_{m,c} + P_t\left(\mathbf{P}_k^i\right)$ contains the RS transmit power $P_t\left(\mathbf{P}_k^i\right) \triangleq Tr\left(\mathbf{P}_k^i\mathbf{P}_k^{i^H}\right) = \left\|\mathbf{p}_k^{i,c}\right\|^2 + \sum_{n=1}^{N_k}\left\|\mathbf{p}_{n,k}^{i,p}\right\|^2$ as well as the mechanical and circuit power consumption $P_{m,c}$. In addition, $\mathcal{U}_{n,k}^i \in \{0,1\}$ is a binary indicator, which represents whether the n-th user of the i-th UAV-cell occupied the k-th SC. Considering all users and SCs, the total SEE is defined

[9]Here, $\alpha_{n,k}^i$ is simply used to show that each user has a share of the common message and has no effect on our SEE equations.

as:

$$\eta_{SEE}^{tot} \triangleq \sum_{i=1}^{I}\sum_{k=1}^{K}\sum_{n=1}^{2}\frac{\mathcal{U}_{n,k}^{i}C_{sec,n,k}^{i,tot}}{P_{tot}\left(\mathbf{P}_{k}^{i}\right)}. \tag{21}$$

Given the constraints imposed, below we aim for maximizing η_{SEE}^{tot} by optimally allocating the limited resources, including the user association matrix $\{\mathbf{U}_i\}_{\forall i}$, the RS TPC $\left\{\mathbf{P}_k^i\right\}$, time slot sharing θ, and power budget $\left\{p_k^i\right\}_{\forall i,k}$.

D. Constraints

The SEE optimization of the RS-aided UAV-HetNet relying on imperfect E-CSIT should consider the following constraints:

- *Power constraints*: The RS TPC at UAV_i must ensure that the transmit power $P_t\left(\mathbf{P}_k^i\right)$ does not exceed the power allocated to SC_k, i.e., p_k^i. On the other hand, the various powers p_k^i assigned to different SC_k have to meet the power limit P_{UAV}^i of UAV_i. In mathematical terms we have:

$$0 \leq P_t\left(\mathbf{P}_k^i\right) \leq p_k^i, \quad \forall k \in \{1,\ldots,K\}, \tag{22}$$

$$\sum_{k=1}^{K} p_k^i \leq P_{UAV}^i.$$

- *Secrecy policy constraints*: We considered the complex secrecy scenario in which the transmitter sides adjust their strategy based on the imperfectly estimated E-CSIT, while Eve aims for increasing its wiretapping capability by accurately estimating the real CSI. The secrecy policy considered has to optimize the RS TPC for ensuring that even the best channel capacity that may be achieved by Eve must fail to support the minimum required common transmission rate $r_k^{i,c}$. Furthermore, we have to ensure that $s_k^{i,c}$ is detectable by both legitimate users. Hence, we must satisfy:

$$\max_{\Lambda_{e,k}^i} C_{e,k}^{i,c} \leq r_k^{i,c}, \tag{23}$$

$$r_k^{i,c} \leq C_k^{i,c},$$

where we have $\Lambda_{e,k}^i \triangleq \Big\{\forall \Delta f_{e,k}^i \in \mathbf{\Theta}_{f_e}, \ \forall \mathbf{\Delta n}_{e,k}^i \in \mathbf{\Theta}_{\mathbf{h}_e}\Big\}$.

- *HetNet communications constraint*: As the MUs have higher priority for using the spectrum, we expect that the total CCI incurred by the I number of UAV-cells is kept below the maximum tolerable interference level I_k of:

$$\sum_{i=1}^{I} p_k^i \left\|\mathbf{h}_{i,k}^M\right\|^2 \leq I_k, \quad \forall k, \tag{24}$$

where $\mathbf{h}_{i,k}^M \in \mathbb{C}^K$ is the corresponding CSI of the link spanning from UAV_i to the M-th macro-user on SC_k.

- *User association constraints*: On one hand, each user occupies one SC_k for each transmission slot. On the other hand, to take full advantage of CRS technique, one pair of CCU and CEU is required for each transmission slot and thus each SC_k is assigned to two users. Based on the above discussions, the user association constraints are given by:

$$\mathcal{U}_{n,k}^i \in \{0,1\}, \quad \forall n,k,i \tag{25}$$

$$\sum_{k=1}^{K}\mathcal{U}_{n,k}^i = 1, \qquad \forall n,i$$

$$\sum_{n=1}^{2}\mathcal{U}_{n,k}^i = 2, \qquad \forall k,i.$$

IV. Joint Resource Allocation and User Association Problem

Under imperfect E-CSIT, the performance of the Tx beamformer $\hat{\mathbf{p}}_z$ is degraded and some AN is leaked to $U_{2,k}^i$. To mitigate this leakage, the proposed robust design maximizes the worst-case ASR. Given this together with the constraints described in (22)-(25), the joint resource allocation and user association scheme relying on the proposed robust SEE maximization is formulated as follows:

$$\max_{\{\mathbf{U}_i\}_{\forall i},\left\{p_k^i\right\}_{\forall i,k},\left\{\boldsymbol{\chi}_k^i\right\}_{\forall i,k}} \left(\min_{\left\{\Lambda_{e,k}^i\right\}_{\forall i,k}} \left(\eta_{SEE}^{tot}\right)\right) \tag{26}$$

s.t.

$$C_1: (22)\text{-}(25), \qquad C_2: 0<\theta\leq 1,$$
$$C_3: 0 \leq p_{k,R}^i \leq \bar{P}_R,\ 0 \leq p_{k,J}^i \leq \bar{P}_J,$$
$$0 \leq p_{k,R}^i + p_{k,J}^i \leq \bar{P}_{max}^{(2)},$$

where $\boldsymbol{\chi}_k^i \triangleq \left(\mathbf{P}_k^i,\ \theta, p_R, p_J\right)$, and $\mathbf{U}_i \triangleq \left[\mathcal{U}_{n,k}^i\right]_{N_{\max}^i \times K}$ is the user association matrix, including the indices of the user-pairs among the $N_{\max}^i$ users and K SCs.

Problem (26) is non-convex due to the non-linear fractional form of the objective function and owing to the discontinuous variable $\mathbf{U}_i$. To circumvent these difficulties, we consider a decomposition based approach, where the NPAP is solved while the user association is carried out.

The NPAP is solved by iterating between the PCP and ICOP steps. To elaborate a little further, during finding $\mathbf{U}_i$ by our user association algorithm, we can optimize the resources, including both the power allocated to each SC $\left\{p_k^i\right\}_{\forall i,k}$, and the network's parameters gathered in $\left\{\boldsymbol{\chi}_k^i\right\}_{\forall i,k}$. To visualize the proposed approach, the whole procedure is shown in Algorithm 1, while further details will be presented in the sequel.

A. User Association

The assignment of SCs can be considered as a two-sided matching procedure relying on the preference lists of both the SCs and users. To expound a little further, first we assume that there are N_{max}^i users and K SCs in the i-th UAV cell, where UAV_i has perfect knowledge of the legitimate CSIT. In this context, each SC may be matched with N_k users, but each user may only be matched with a single SC. In order to conceive a low-complexity matching procedure, each SC can be occupied by a maximum of $N_k = 2$ users.

In the two-sided matching algorithm, first each user $U_{n,k}^i$ will initialize its own preference list of SCs based on the channel quality $\mu_{n,k}^i \triangleq \frac{\left\|\mathbf{h}_{n,k}^i\right\|}{\left\|\hat{\mathbf{h}}_{e,k}^i\right\|}$. Once each user user has constructed its preference list, a matching request will be sent to the SCs, and then the user $U_{n,k}^i$ as well as the preferred SC_k may form a matching pair. If the number of users that prefer SC_k is less

than N_k, SC_k can still accommodate further requests and be matched with additional users, until it becomes completely filled. Otherwise, N_k number of users from those that prefer SC_k and succeed in increasing their SEE by camping on SC_k will be chosen and then SC_k rejects the remaining requests. To arrange for this, based on the preference list of users on each SC_k, ICOP is called and those users that maximize $\eta_{SEE_k^i}$ are assigned to SC_k as the optimal match. The rejected users are then collected in the so-called unmatched list and initiate their new contention for the remaining SC_k. This process will be continued until no users remain in the unmatched list. The first part of the assignment ends here, yielding a preliminary SC matching $\mathbf{U}_i$ for each UAV cell. Now, given the resultant $\{\mathbf{U}_i\}_{\forall i}$ and $\left\{\boldsymbol{\chi}_k^i\right\}_{\forall i,k}$, we optimize the power $\left\{p_k^i\right\}_{\forall k,i}$ allocated to each SC, through the PCP. Again, given the improved values $\left\{p_k^{i\,[l]}\right\}_{\forall k,i}$, we repeat the previous steps and this iterative process continues until convergence is attained. In particular, the l-th iteration of the overall algorithm is constituted by separately minimizing the criterion with respect to each of $\left[\{\mathbf{U}_i\}_{\forall i}, \left\{\boldsymbol{\chi}_k^i\right\}_{\forall i,k}\right]$ and $\left\{p_k^i\right\}_{\forall k,i}$, while keeping the other one fixed.

It should be pointed out that the above-mentioned process will result in a sub-optimal solution. To improve the result, the above-mentioned procedure is followed by a swapping procedure. This swapping process includes exchanging two users, which have already been matched with the sub-channels SC_k through the two-sided matching procedure. During this swapping process, the following points must be considered:

- At each time, the swapping process is performed only between two users on different SCs, while keeping the state of other users assigned to SCs without changing the state of any other user already matched to SCs.
- The swapping process aims for enhancing the achievable SEE. Thus if two users form a swapping pair, the SEE of at least one of them will have a promotion and the SEE corresponding to the other one participating in the swapping process is not decreased.

According to the above conditions, matched users search over other SCs to form a swapping pair. The number of swappings between two users cannot exceed $N_k = 2$ in order to prevent unnecessary looping.

B. Intra-Cell Optimization Problem (ICOP)

Based on the previous section, we first carry out two-sided matching. Explicitly, we have to select the best user pair, which maximizes the SEE achieved through each SC_k at UAV_i, i.e., $\eta_{SEE_k^i}$, by finding $\boldsymbol{\chi}_k^i$. Given the power of each SC, $p_k^{i\,[l]}$ determined by the PCP from the previous iteration, and initialized by $\left\{p_k^{i\,[0]}\right\}_{\forall i,k} = \frac{P_{UAV}^i}{K}$, the following optimization problem must be solved at this stage:

$$\max_{\boldsymbol{\chi}_k^i} \left(\eta_{SEE_k^i}\right),\ \left\{\forall \Lambda_{e,k}^i\right\} \quad (27)$$

s.t.

$$C_1 : 0 \leq Tr\left(\mathbf{P}_k^i \mathbf{P}_k^{i^H}\right) \leq p_k^{i^{[l]}},$$

$$C_2 : (22), (23).$$

Problem (27) is still non-convex because of the non-convex objective function (OF) as well as non-convex constraint set. To circumvent the non-convexity, we rely on the SPCA. Prior to applying SPCA, we have to relax the OF as well as the constraints as much as possible by variable transformation and linearization. Then, using the SPCA, we adopt an iterative solution, where the non-convex factor at each iteration is approximated by its first-order Taylor expansion. Given this perspective, we first attempt to circumvent the non-convexity imposed by the fractional form and logarithmic function of the OF by introducing two sets of auxiliary variables, namely $\mathbf{f}_k^i \triangleq \left[f_{k,0}^i, f_{k,1}^i, .., \ f_{k,N_k}^i\right]$ and $\mathbf{g}_k^i \triangleq \left[g_{k,0}^i, g_{k,1}^i, ..., \ g_{k,N_k}^i\right]$. The vector $\mathbf{f}_k^i$ includes the corresponding auxiliary variables to describe the rates of the common and private streams at the legitimate users, namely $f_{k,0}^i = C_k^{i,c}, f_{k,n}^i = C_{n,k}^{i,p}$, while $\mathbf{g}_k^i$ is used for describing the relevant rates at the Eve, i.e., $g_{k,0}^i = C_{e,k}^{i,c}$, $g_{k,n}^i = C_{e,n,k}^{i,p}$. Using this variable transformation, the OF can be recast as:

$$\eta_{SEE_k^i} = \frac{\overbrace{\left(C_k^{i,c} + \sum_{n=1}^{N_k} C_{n,k}^{i,p}\right)}^{Part\,I} - \overbrace{\left(C_{e,k}^{i,c} + \sum_{n=1}^{N_k} C_{e,n,k}^{i,p}\right)}^{Part\,II}}{P_{tot}\left(\mathbf{P}_k^i\right)} \quad (28)$$
$$= \frac{f_{k,0}^i - g_{k,0}^i + \sum_{n=1}^{N_k}\left(f_{k,n}^i - g_{k,n}^i\right)}{P_{tot}\left(\mathbf{P}_k^i\right)},$$

where it is assumed that $f_{k,n}^i \geq g_{k,n}^i,\ \forall n \in \{0, 1, 2, .., N_k\}$. Now, with the objective of linearization and getting rid of the fractional form, we can replace the Problem (27) by exploiting the following theorem:

Theorem 2. *The optimal $\eta_{SEE_k^i}^*$ for (27) can be acquired through the following optimization problem if and only if $f\left(\eta_{SEE_k^i}^*\right) = 0$:*

$$f\left(\eta_{SEE_k^i}\right) \triangleq \max_{\boldsymbol{\pi}_k^i, \Lambda_{e,k}^i} \left\{\sum_{n=0}^{N_k}\left(f_{k,n}^i - g_{k,n}^i\right) - \right. \quad (29)$$
$$\left. \eta_{SEE_k^i}\left(P_m + \left\|\mathbf{p}_k^{i,c}\right\|^2 + \sum_{n=1}^{N_k}\left\|\mathbf{p}_{n,k}^{i,p}\right\|^2\right)\right\},$$

s.t.

$$C_1 : f_{k,0}^i \leq C_k^{i,c}, \qquad C_2 : f_{k,n}^i \leq C_{n,k}^{i,p},\ \forall n,$$

$$C_3 : g_{k,0}^i \geq \max_{\Lambda_{e,k}^i} C_{e,k}^{i,c}, \qquad C_4 : g_{k,n}^i \geq \max_{\Lambda_{e,k}^i} C_{e,n,k}^{i,p},$$

$$C_5 : 0 \leq Tr\left(\mathbf{P}_k^i \mathbf{P}_k^{i^H}\right) \leq p_k^{i\,[l]}, \qquad C_6 : \beta_k^i \geq \frac{P_t\left(\mathbf{P}_k^i\right)}{p_k^{i\,[l]}}$$

$$C_7 : f_{k,n}^i \geq g_{k,n}^i, \forall n \in \{0, 1, .., N_k\},$$

$$C_8 : r_k^{i,c} \leq f_{k,0}^i,\ r_k^{i,c} \geq g_{k,0}^i$$

$$C_9 : \textit{(26-}C_2\textit{), (26-}C_3\textit{)}$$

where $\boldsymbol{\pi}_k^i \triangleq \left[\ \mathbf{P}_k^i, \theta, p_{k,R}^i, p_{k,J}^i, \mathbf{f}_k^i, \mathbf{g}_k^i, \beta_k^i\right]$.

Proof:

please see Appendix A.

■

Based on Theorem 2, we present a two-tier iterative algorithm to attain the ξ-optimal solution. More explicitly, the $(m+1)$-st iteration of the outer tier consists of calculating $\eta_{SEE_k^i}^{[m+1]}$ by substituting the optimal point $\boldsymbol{\pi}_k^{i*}$ calculated in the inner tier as follows:[10]

$$\begin{gathered}\boldsymbol{\pi}_k^{i*} \text{ obtained from } f^{[*]}\left(\eta_{SEE_k^i}^{[m]}\right)=0 \\ \Downarrow \\ \text{update } \eta_{SEE_k^i}^{[m+1]}=\frac{f_{k,0}^{i}{}^{*}-g_{k,0}^{i}{}^{*}+\sum\limits_{n=1}^{N_k}\mathcal{U}_{n,k}^{i}\left(f_{k,n}^{i}{}^{*}-g_{k,n}^{i}{}^{*}\right)}{P_{tot}\left(\mathbf{P}_k^{i}{}^{*}\right)},\end{gathered} \tag{30}$$

where the superscript "$*$" represents the final iteration of the inner tier. Then, the outer tier proceeds to the next iteration and runs until $\left|\eta_{SEE_k^i}^{[m+1]}-\eta_{SEE_k^i}^{[m]}\right|\leq\xi$ is met or the maximum affordable number of iterations m_{max} is reached. To find the ξ-optimal solution $\boldsymbol{\pi}_k^{i*}$, the problem (29) is solved using SPCA in another iterative process in the inner tier. In particular, the inner iterations are continued until the stopping criterion $\left|f^{[t+1]}\left(\eta_{SEE_k^i}^{[m]}\right)-f^{[t]}\left(\eta_{SEE_k^i}^{[m]}\right)\right|\leq\delta_I$ is satisfied at the $(t+1)$-st iteration or the maximum affordable number of iterations t_{max} is reached. The proposed two tier ICOP scheme is presented in Algorithm 2. In order to handle the constraints (29-C_1 : C_9), we further define the sets of new auxiliary variables$\boldsymbol{\beta}_c \triangleq \left[\beta_{c,1}^{(1)},\beta_{c,2}^{(1)},\beta_{c,2}^{(2)},\beta_{c,e}^{(1)},\beta_{c,e}^{(2)}\right]$, $\boldsymbol{\rho}_c \triangleq \left[\rho_{c,1}^{(1)},\rho_{c,2}^{(1)},\rho_{c,2}^{(2)},\rho_{c,e}^{(1)},\rho_{c,e}^{(2)}\right]$, $\boldsymbol{\beta}_p \triangleq [\beta_{p,1},\beta_{p,2},\beta_{1,e},\beta_{2,e}]$, $\boldsymbol{\rho}_p \triangleq [\rho_{p,1},\rho_{p,2},\rho_{1,e},\rho_{2,e}]$, $\boldsymbol{\pi}_{c,e} \triangleq [x_{c,e},\ y_{c,e},\ u_{1,c,e},\ u_{2,c,e},v_{c,e},\ d_{c,e},\ f_{c,e}]$. Accordingly, we can deal with each non-convex constraint independently to attain its equivalent convex counterpart. Based on the above discussions on SPCA, we first aim for eliminating the non-convexity by variable transformation and linearization. If the non-convexity persists, we approximate the non-convex factor at each iteration by its first-order Taylor expansion. Using this technique, the affine approximation becomes straightforward for most of the constraints. However, for gaining better insight concerning the procedure we have detailed the mathematical analysis of (26-C_1) and (26-C_3) respectively in Appendices B and C, and due to space constraint we avoid to bring the similar procedure for (26-C_2) and (26-C_4). Hence now, we can replace each non-convex constraint by its affine approximation. Using these approximations together with $\eta_{SEE_k^i}^{[m]}$ gleaned from the outer tier, the $(t+1)$-st iteration of the inner tier solves the following convex optimization problem for calculating the ξ-optimal $\boldsymbol{\pi}_k^{i\,[t+1]}$ as follows:

$$\begin{aligned}\boldsymbol{\pi}_k^{i\,[t+1]}=\arg\max_{\boldsymbol{\pi}_k^i}\Bigg\{&f_{k,0}^{i}-g_{k,0}^{i}+\sum_{n=1}^{N_k}\mathcal{U}_{n,k}^{i}\left(f_{k,n}^{i}-g_{k,n}^{i}\right)\\&-\eta_{SEE_k^i}^{[m]}\left(P_m+\beta_k^i\,p_k^{i\,[l]}\right)\Bigg\}\end{aligned} \tag{31}$$

s.t.

$C_1: f_{k,0}^{i}\leq C_k^{i,c}\Leftrightarrow$

I. $\Theta^{[t]}\left(\theta,\beta_{c,1}^{(1)}\right)\geq f_{k,0}^{i}$,

II. $\Theta^{[t]}\left(\theta,\beta_{c,2}^{(1)}\right)+\Theta^{[t]}\left(1-\theta,\beta_{c,2}^{(2)}\right)\geq f_{k,0}^{i}$,

III. $\left|\left(\mathbf{h}_{n,k}^{i}\right)^H\mathbf{p}_{1,k}^{i,p}\right|^2+\left|\left(\mathbf{h}_{n,k}^{i}\right)^H\mathbf{p}_{2,k}^{i,p}\right|^2+\delta^2$ $P_k^M\left\|\mathbf{c}_{n,k}^{i}\right\|^2-\Psi^{[t]}\left(\mathbf{p}_k^{i,c},\rho_{c,n}^{(1)};\,\mathbf{h}_{n,k}^{i}\right)\leq 0$,

IV. $p_{k,J}^{i}\left|\left(\mathbf{h}_{2,k}^{i}\right)^H\hat{\mathbf{p}}_{k,z}^{i}\right|^2+P_k^M\left\|\mathbf{c}_{2,k}^{i}\right\|^2+\delta^2-$ $\Psi^{[t]}\left(\delta_{k,R}^{i},\rho_{c,2}^{(2)};\,f_{1,2,k}^{i}\right)\leq 0$,

V. $1+\rho_{c,1}^{(1)}-2^{\beta_{c,1}^{(1)}}\geq 0$,

VI. $1+\rho_{c,2}^{(j)}-2^{\beta_{c,2}^{(j)}}\geq 0$,

$C_2: f_{k,n}^{i}\leq C_{n,k}^{i,p}\Leftrightarrow$

I. $\Theta^{[t]}\left(\theta,\beta_{p,n}\right)\geq f_{k,n}^{i},\ n\in\{1,2\}$

II. $\left|\left(\mathbf{h}_{n,k}^{i}\right)^H\mathbf{p}_{j,k}^{i,p}\right|^2+P_k^M\left\|\mathbf{h}_{n,k}^{M,i}\right\|^2+\delta^2-$ $\Psi^{[t]}\left(\mathbf{p}_{n,k}^{i,p},,\rho_{p,n};\mathbf{h}_{n,k}^{i}\right)\leq 0,\ n\neq j$,

III. $1+\rho_{p,n}-2^{\beta_{p,n}}\geq 0$,

$C_3: g_{k,0}^{i}\geq\max_{A_{e,k}^{i}}C_{e,k}^{i,c}\Leftrightarrow$

I. $\bar{\Theta}^{[t]}\left(\theta,\beta_{c,e}^{(1)}\right)+\bar{\Theta}^{[t]}\left(1-\theta,\beta_{c,e}^{(2)}\right)\leq\alpha_{c,e}$,

II. $\alpha_{c,e}\leq r_k^{i,c}$,

III. $\sum_{n=1}^{2}u_{n,c,e}+P_k^M\left\|\mathbf{c}_{e,k}^{i}\right\|^2+\delta^2\geq d_{c,e}$,

IV. $\frac{x_{c,e}^2}{d_{c,e}}\leq\rho_{c,e}^{(1)}$,

V. $v_{c,e}+P_k^M\left\|\mathbf{c}_{e,k}^{i}\right\|^2+\delta^2\geq f_{c,e}$,

VI. $\frac{y_{c,e}^2}{f_{c,e}}\leq\rho_{c,e}^{(2)}$,

VII. $\left|\left(\hat{\mathbf{h}}_{e,k}^{i}\right)^H\mathbf{p}_k^{i,c}\right|+\sqrt{N_t\epsilon}\left\|\mathbf{p}_k^{i,c}\right\|_2\leq x_{c,e}$

VIII. $Tr\left[\left(\hat{\mathbf{H}}_{e,k}^{i}-\xi_e\mathbf{I}\right)\mathbf{P}_{n,k}^{i,p}\right]\geq u_{n,c,e}$,

IX. $\delta_{k,R}^{i}\left(\sqrt{\epsilon}+\left|\hat{g}_{1,e,k}^{i}\right|\right)\leq y_{c,e}$,

X. $p_{k,J}^{i}Tr\left[\left(\hat{\mathbf{H}}_{e,k}^{i}-\xi_e\mathbf{I}\right)\mathbf{P}_{k,z}^{i,c}\right]\geq v_{c,e}$

XI. $1+\rho_{c,e}^{(j)}-\Gamma^{[t]}\left(\beta_{c,e}^{(j)}\right)\leq 0, j\in\{1,2\}$

[10] Note that $f^{[*]}\left(\eta_{SEE_k^i}^{[m]}\right)$ represents the value of $f\left(\eta_{SEE_k^i}^{[m]}\right)$ at the point of $\boldsymbol{\pi}_k^{i\,[*]}$.

$C_4: g_{k,n}^i \geq \max_{\Lambda_{e,k}^i} C_{e,n,k}^{i,p}$,

I. $\bar{\Theta}^{[t]}(\theta, \beta_{n,e}) \leq g_{k,n}^i$,

II. $\frac{x_{n,e}^2}{d_{n,e}} \leq \rho_{n,e}$,

III. $\left|\left(\hat{\mathbf{h}}_{e,k}^i\right)^H \mathbf{p}_{n,k}^{i,p}\right| + \sqrt{N_t}\epsilon \left\|\mathbf{p}_{n,k}^{i,p}\right\|_2 \leq x_{n,e}$

IV. $u_{c,c,e} + u_{j,c,e} + P_k^M \left\|\mathbf{c}_{e,k}^i\right\|^2 + \delta^2 \geq d_{n,e}, j \neq n$

V. $Tr\left[\left(\hat{\mathbf{H}}_{e,k}^i - \xi_e \mathbf{I}\right)\mathbf{P}_k^{i,c}\right] \geq u_{c,c,e}$,

VI. $1 + \rho_{n,e} - \Gamma^{[t]}(\beta_{n,e}) \leq 0$,

$C_5: 0 \leq Tr(\mathbf{P}_k^i \mathbf{P}_k^{i\,H}) \leq {p_k^i}^{[l]}, \quad \forall i,k$

$C_6: \frac{\|\mathbf{p}_k^{i,c}\|^2 + \sum_{n=1}^{N_k} \|\mathbf{p}_{n,k}^{i,p}\|^2}{{p_k^i}^{[l]}} \leq \beta_k^i$

$C_7: f_{k,n}^i \geq g_{k,n}^i, \forall n \in \{0,1,..,N_k\}$,

$C_8: f_{k,0}^i \geq r_k^{i,c}$

Algorithm 2 Proposed ξ-optimal ICOP

Function *Outer_Iteration*

Step 1: Initialize the maximum number of iterations m_{max}, t_{max} and the maximum tolerance ξ.

Step 2: Initialize $\eta_{SEE_k^i}^{[0]} = 0$ and the outer iteration index $m = 0$.

While $\left(\left|\eta_{SEE_k^i}^{[m+1]} - \eta_{SEE_k^i}^{[m]}\right| \geq \xi \text{ or } m \leq m_{max}\right)$ do:

Step 3: Call the **Function** *Inner_Iteration* with $\eta_{SEE_k^i}^{[m]}$ to obtain the ξ-optimal solution ${\boldsymbol{\pi}_k^i}^*$.

Step 4: Update $\eta_{SEE_k^i}^{[m+1]} = \frac{{f_{k,0}^i}^* - {g_{k,0}^i}^* + \sum_{n=1}^{N_k} \mathcal{U}_{n,k}^i \left({f_{k,n}^i}^* - {g_{k,n}^i}^*\right)}{P_{tot}\left({\mathbf{P}_k^i}^*\right)}$.

Step 5: **Goto** Step 3.

end while.

Step 6: Return the ξ-optimal solution ${\boldsymbol{\pi}_k^i}^*$ and $\eta_{SEE_k^i}^* = \eta_{SEE_k^i}^{[m+1]}$.

end.

==========

Function *Inner_Iteration* $\left(\eta_{SEE_k^i}^{[m]}\right)$

Step 1: Initialize the inner iteration index $t = 0$, ${\boldsymbol{\pi}_k^i}^{[0]}$ and $f^{[0]}\left(\eta_{SEE_k^i}^{[m]}\right) = 0$.

While $\left(\left|f^{[t+1]}\left(\eta_{SEE_k^i}^{[m]}\right) - f^{[t]}\left(\eta_{SEE_k^i}^{[m]}\right)\right| \geq \xi \text{ or } t \leq t_{max}\right)$ do:

Step 2: Find the ξ-optimal solution ${\boldsymbol{\pi}_k^i}^{[t+1]}$ of the following problem for given ${\boldsymbol{\pi}_k^i}^{[t]}$, $\left\{{p_k^i}^{[l]}\right\}_{\forall i,k}$ and $\eta_{SEE_k^i}^{[m]}$:

$${\boldsymbol{\pi}_k^i}^{[t+1]} = \text{Solving } (31),$$

Step 3: Update $f^{[t+1]}\left(\eta_{SEE_k^i}^{[m]}\right) = \sum_{n=0}^{N_k}\left({f_{k,n}^i}^{[t]} - {g_{k,n}^i}^{[t]}\right) - \eta_{SEE_k^i}^{[m]}\left(P_m + \beta_k^{i\,[t]} {p_k^i}^{[l]}\right)$.

Step 4: **Goto** Step 2.

end while.

Step 5: Return ${\boldsymbol{\pi}_k^i}^* = {\boldsymbol{\pi}_k^i}^{[t+1]}$.

end

$C_9: r_k^{i,c} \leq f_{k,0}^i,\ r_k^{i,c} \geq g_{k,0}^i$

$C_{10}: 0 < \theta \leq 1$,

$C_{11}: 0 \leq p_{k,R}^i \leq \bar{P}_R,\ 0 \leq p_{k,J}^i \leq \bar{P}_J,$
$0 \leq p_{k,R}^i + p_{k,J}^i \leq \bar{P}_{max}^{(2)}$,

where $\xi_e = N_t\epsilon + 2\sqrt{N_t}\epsilon \left\|\hat{\mathbf{h}}_{e,k}^i\right\|_2$, $\hat{\mathbf{H}}_{e,k} \triangleq \mathbf{h}_{e,k}^i {\mathbf{h}_{e,k}^i}^H$, $\mathbf{P}_{n,k}^{i,p} \triangleq \mathbf{p}_{n,k}^{i,p} {\mathbf{p}_{n,k}^{i,p}}^H$, $\mathbf{P}_k^{i,c} \triangleq \mathbf{p}_k^{i,c} {\mathbf{p}_k^{i,c}}^H$, $\mathbf{P}_{k,z}^i \triangleq \hat{\mathbf{p}}_{k,z}^i \left(\hat{\mathbf{p}}_{k,z}^i\right)^H$, $\sqrt{P_{k,R}^i} \triangleq \delta_{k,R}^i$, $\Theta^{[m]}(x,y) \triangleq \frac{1}{2}(x^{[m]} + y^{[m]})\ (x+y) - \frac{1}{4}(x^{[m]} + y^{[m]})^2 - \frac{1}{4}(x-y)^2$, $\bar{\Theta}^{[m]}(x,y) \triangleq \frac{1}{4}(x+y)^2 + \frac{1}{4}(x^{[m]} - y^{[m]})^2 - \frac{1}{2}(x^{[m]} - y^{[m]})\ (x-y)$, $\Psi^{[m]}(\mathbf{u}, x; \mathbf{h}) \triangleq \frac{2\Re e\left\{\left(\mathbf{u}^{[m]}\right)^H \mathbf{h}\mathbf{h}^H \mathbf{u}\right\}}{x^{[m]}} - \frac{\left|\mathbf{h}^H \mathbf{u}^{[m]}\right|^2 x}{\left(x^{[m]}\right)^2}$, $\Omega^{[m]}(\mathbf{u}, \mathbf{v}; \mathbf{h}) \triangleq \Psi^{[m]}(\mathbf{u}, 1; \mathbf{h}) - \Psi^{[m]}(\mathbf{v}, 1; \mathbf{h})$, and $\Gamma^{[m]}(x) \triangleq 2^{x^{[m]}}\left[1 + \ln(2)\left(x - x^{[m]}\right)\right]$.

Algorithm 3 Overall proposed ξ-optimal algorithm

Step 1: At the first iteration equal powers are assigned to different SCs, i.e., ${p_k^i}^{[0]} = \frac{P_{UAV}}{K}$, and first iteration index $l = 0$.

While $\left(\min_{i,k}\left(\left|{p_k^i}^{[l+1]} - {p_k^i}^{[l]}\right|\right) \geq \xi \text{ or } l \leq L_{max}\right)$ do:

Step 2: Call the **Two-sided matching** algorithm using **ICOP** with ${p_k^i}^{[l]}$ to obtain the ξ-optimal solution $\left\{{\boldsymbol{\pi}_k^i}^*, \eta_{SEE_k^i}^*\right\}_{\forall i,k}$ and $\{\mathbf{U}_i\}_{\forall i}$.

Step 3: Find the optimal solution $\left\{{p_k^i}^{[l+1]}\right\}_{\forall i,k}$ of problem (32) for a given $\left(\left\{{\boldsymbol{\pi}_k^i}^*, \eta_{SEE_k^i}^*\right\}_{\forall i,k}, \{\mathbf{U}_i\}_{\forall i}\right)$.

Step 4: **Goto** Step 2.

end while.

Step 5: Call the **Swapping** algorithm.

Step 6: Obtain the optimal solution $\left\{{p_k^i}^*\right\}_{\forall i,k} = \left\{{p_k^i}^{[l+1]}\right\}_{\forall i,k}$.

end.

C. Power Control Problem (PCP)

Now given the optimal $\left\{{\boldsymbol{\pi}_k^i}^*, \eta_{SEE_k^i}^*\right\}_{\forall i,k}$ obtained from the ICOP, and $\{\mathbf{U}_i\}_{\forall i}$ obtained from the two-sided matching algorithm, the $(l+1)$-st iteration of PCP comprises the following convex optimization problem:

$$\left\{{p_k^i}^{[l+1]}\right\} = \arg\max_{\{p_k^i\}} \left\{\sum_{n=0}^{2}\left({f_{k,n}^i}^* - {g_{k,n}^i}^*\right) - \eta_{SEE_k^i}^*\left(P_m + {\beta_k^i}^* {p_k^i}^*\right)\right\},\ \forall k \tag{32}$$

s.t.

$C_1: 0 \leq Tr(\mathbf{P}_k^{i\,*}\left(\mathbf{P}_k^{i\,*}\right)^H) \leq p_k^i, \quad \forall i,k$

$C_2: \frac{P_t\left(\mathbf{P}_k^{i\,*}\right)}{p_k^i} \leq {\beta_k^i}^*$

$C_3: \sum_{k=1}^{K} p_k^i \leq P_{UAV}$

$$C_4 : \sum_{i=1}^{I} p_k^i \left\| \mathbf{h}_{i,k}^M \right\|^2 \leq I_k, \quad \forall k$$

Based on the solutions acquired by PCP and ICOP, the overall procedure is summarized in Algorithm 3.

V. Complexity Analysis

The overall SPCA-based algorithm includes three steps of user association the intra-cell optimization problem (ICOP) and power control problem (PCP). Regarding the user association, the optimal match for all users and subchannels is acquired through exhaustive search whose complexity is $\mathcal{O}_{exh} = \mathcal{O}(\frac{N!}{2^K})$ for $N = 2K$ number of users and K number of sub-channels. By contrast, in the proposed two-sided matching, which involves the SPCA, the worst-case situation occurs when each user pairs has to compare its achieved performance to that of a previous pair, for the entires set of subchannels. Even in this worst-case scenario the complexity does not exceed $\mathcal{O}_{two-sided} = \mathcal{O}(K^2)$. Thus, if the Logarithmic form is used to represent the computational complexities, we have $\mathcal{O}_{two-sided} = \mathcal{O}(\ln K) \leq \mathcal{O}_{exh} = \mathcal{O}(\ln((2K)!)) = \mathcal{O}(\ln((2K)! - K))$, which suggests that our proposed two-sided matching could substantially reduce the computational complexity. Now regarding the computational complexity of PDP in (7), this optimization problem is a semidefinite program (SDP), whose constraints were transformed into first-order Taylor convex approximations. Even though it is not a standard SDP problem [41], using the interior-point method, the worst-case complexity can be calculated as $\mathcal{O}\left(m^2 \left(\sum_i m_i^2\right) \sqrt{\sum_i m_i}\right)$, where m is the number of optimization variables and m_i is the dimension of the i-th semidefinite cone [41]. Therefore, when the interior-point method is employed to solve the problem (7), the worst-case computational complexity at each iteration can be calculated by $\mathcal{O}_{SPCA} = \mathcal{O}\left((N-1)^2 \left(2\left(\sqrt{2}N\right)^2\right) \sqrt{2(N)^2 + 2}\right)$.

VI. Simulation Results

In this section, we present numerical results for characterizing our proposed framework using the following simulation setting, unless stated otherwise. The BS is arranged at the center of a macro-cell having a radius of $R_{BS} = 1500$ m, where $N_M = 4$ macro users are randomly distributed in the DL coverage area of the BS. In the scenario investigated several UAVs randomly move above the users and hover to provide communication services. Explicitly, $I = 3$ UAVs are randomly distributed within the macro cell and they have a coverage radius of $R_{UAV} = 400$ m and altitude of $H_i = 200$ m. Each UAV has a minimum distance constraint from the ground BS for ensuring that the UAV can serve users also at the edge of the macro-cell with the aid of $K = 4$ SCs. Furthermore, the users are randomly located within the coverage area of each UAV, two legitimate user per each SC_k. The minimum distance between the BS and UAV cells is 50 m on a horizontal plane. In contrast to the channel between the macro BS and the users, the path-loss model in the UAV network includes both LoS and NLoS links associated with the path-loss exponents of $\mathcal{L}_{n,k}^i = 2$ and $\mathcal{N}_{n,k}^i = 3.5$, respectively. We assume that the channel gain of $U_{1,k}^i$ is higher than that of $U_{2,k}^i$. The simulation results are averaged over 10^3 realizations of the proposed scheme. Moreover, we set $N_{max} = M_{max} = 20$ and the maximum tolerable threshold value for the termination of Algorithm 2 is set to the value of $\delta_I = 10^{-2}$. The power of the macro BS is $p_{M,k} = 20$ dBm for each SC. A channel estimation error variance of $\epsilon = 10^{-3}$ and a maximum tolerance of $\xi = 10^{-3}$ is assumed for the termination criterion used in Algorithm 2. The additive noise at the receiver is considered to have a normalized power of $\delta^2 = 1$, and the minimum required transmission rate of the common stream is $r_k^{i,c} = 1$ Bit/sec/Hz.

Fig. 3 illustrates the convergence of the inner-iteration problem for our proposed SEE maximization scheme by portraying the trend of $f(\eta_{SEE_k^i})$ defined in (29). According to our scheme proposed in Algorithm 2, $f(\eta_{SEE_k^i})$ gradually increases with the number ICOP inner iterations denoted by t. This trend may also be seen from Fig. 3. The figure is also plotted for different outer-iteration induces m of ICOP. Accordingly, as the outer-iteration index increases, $\eta_{SEE_k^i}^{[m]}$ gradually converges toward its optimal point $\eta_{SEE_k^i}^*$ (the convergence of $\eta_{SEE_k^i}$ is investigated in the next figure). Then, based on Theorem 2, $f(\eta_{SEE_k^i})$ reaches the maximum value of zero at its optimum point, when substituting $\eta_{SEE_k}^* = \eta_{SEE_k^i}^{[t+1]}$. The above-mentioned trends can be observed from Fig. 3, where upon increasing m results in $\eta_{SEE_k^i}^{[m]}$ converging to zero at its optimal point. Hence, Fig. 3 also validates the method proposed in Theorem 2 for solving the ICOP.

Fig. 4 characterizes the convergence of the outer-iteration problem in Algorithm 2 by investigating the behavior of $\eta_{SEE_k^i}^{[m]}$ for each UAV cell $i \in I$ and each SC_k $k \in K$. As seen from the figure, by harnessing the proposed SEE maximization algorithm, the SEE metric converges to its optimum value for all the SCs in each of the UAV cells, after running Algorithm 2 for a few iterations.

Fig. 5 depicts the optimized SEE η_{SEE}^{tot} of the overall UAV-assisted network versus the UAVs' altitude for different values of channel uncertainties ϵ, regarding the eavesdropping link. Observe from the figure that increasing H_i improves the maximum achievable SEE until reaching the optimal altitude, at which the UAV has complete control over all macro-users. However, any further altitude increase will degrade the secrecy performance, because the UAV should increase its transmit power in order to compensate the path-loss, while maintaining the minimum required QoS $r_k^{i,c}$ for the terrestrial users. Hence, the SEE η_{SEE}^{tot} decays. This fact can be readily seen from (2) together with the formulas of $\gamma_{n,k}^{i,c^{(1)}}$ and $\gamma_{2,k}^{i,c^{(2)}}$ as well. Fig. 5 also shows the effect of channel uncertainties ϵ on the overall SEE of our proposed scheme. We can see that an increased η_{SEE}^{tot} can be attained for more accurate CSI estimates of the potential Eve. However, the effect of ϵ on SEE vanishes for a UAV hovering at a sufficiently high altitude. This is because for high values of H_i, the LoS part of the signals received through the UAV links is more significant than the non-LoS part, which encounters small-scale fading. Therefore, the value of ϵ which corresponds to the small-scale fading becomes less influential in determining η_{SEE}^{tot}.

Fig. 6 shows the optimal SEE, η_{SEE}^{tot}, versus the number N_t of UAV transmit antennas both for our CRS scheme and for its Cooperative Non-Orthogonal Multiple Access (C-NOMA) and for its Cooperative Beamforming (C-BF) counterparts. Explicitly, C-BF simply exploits its angular selectivity as

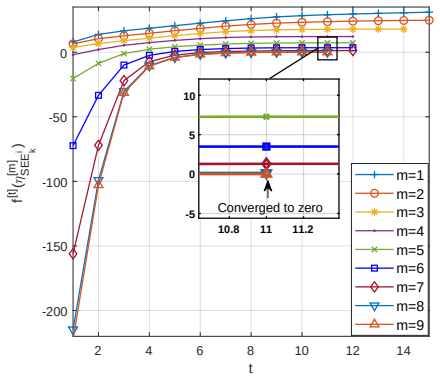

Fig. 3. Convergence of the inner-tier of Algorithm 2

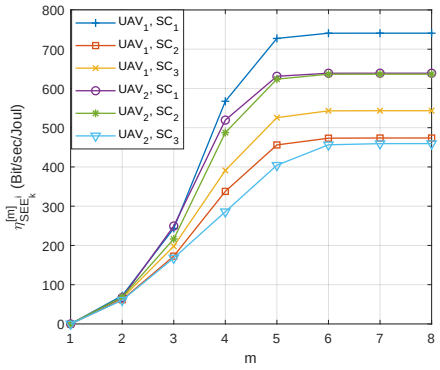

Fig. 4. Convergence of the outer-iteration problem in Algorithm 2

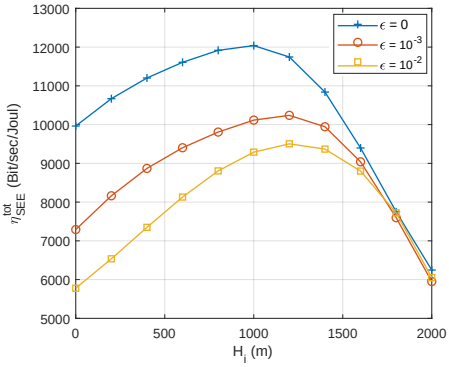

Fig. 5. η_{SEE}^{tot} versus the H_i for different values of channel uncertainties

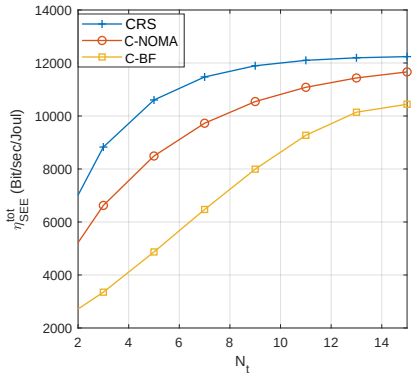

Fig. 6. η_{SEE}^{tot} versus the number of transmitting antennas at UAVs

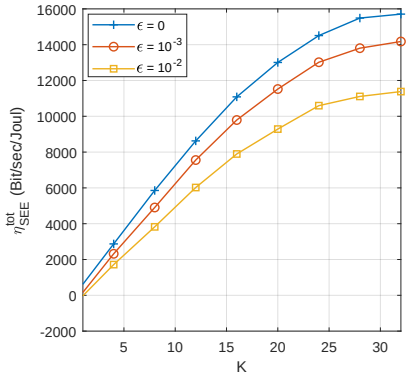

Fig. 7. η_{SEE}^{tot} versus the number of available SCs at each UAV cell

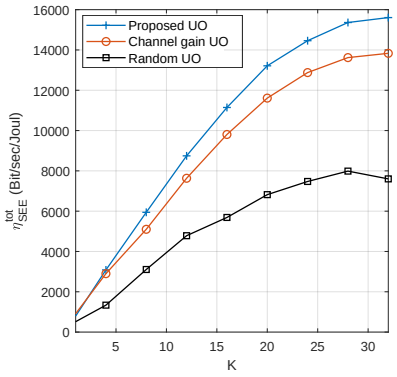

Fig. 8. Performace of proposed user ordering (UO) method compared to other strategies

a PLS technique to guard against Eve at the PHY layer. This scheme relies on allocating no power to the common stream (i.e., $\mathbf{p}_k^{i,c} = \mathbf{0}$), hence $\mathcal{W}_{n,k}^{i,p}$ is encoded directly into $s_{\mathrm{n},k}^{i,p}$. No interference is decoded at the receiver using the common message, and the interference between $s_{1,k}^{i,p}$ and $s_{2,k}^{i,p}$ is fully treated as noise. By contrast, C-NOMA is obtained by encoding $\mathcal{W}_{2,k}^{i,p}$ entirely into $s_k^{i,c}$ (i.e., $\mathcal{W}_k^{i,c} = \mathcal{W}_{2,k}^{i,p}$) and $\mathcal{W}_{1,k}^{i,p}$ into $s_{1,k}^{i,p}$, while turning off $s_{2,k}^{i,p}$ (i.e., $\mathbf{p}_{2,k}^{i,p} = \mathbf{0}$). In this way, CCU fully decodes the interference created by the message of CEU. The mapping of the messages to the streams is further illustrated in Table IV [26], [30]. It is clear from the figure that our proposed CRS scheme outperforms both benchmark techniques in terms of its SEE metric, which is due to the fact that the CRS uses the common message not only to serve as AN for impairing the decoding of the Eve, but also to enhance the interference management between the CCU and CEU. Moreover, it can be inferred from the figure that increasing the number of transmit antennas N_t at the UAV enhances the system's performance by focusing the UAV beams toward the intended legitimate user.

Fig. 7 depicts the optimal SEE, η_{SEE}^{tot}, versus the number of SCs available at each UAV cell. Based on the definition of the overall SEE in (21), one can infer that increasing the number of SCs, which can be equivalently interpreted as increasing the number of users served in UAV cells, results in SEE enhancement. This fact can be seen from the Fig. 7 as well. On the other hand, upon increasing K the optimal SEE saturates, because the total power budget P_{UAV}^{i} of UAVs is limited. Therefore, when K increases, the amount of transmit power allocated to each SC decreases, and it may become insufficient for the QoS of the users supported by the UAVs to be met.

Fig. 8 contrasts the SEE performance of our proposed user ordering method both to the one proposed in [36] and to a purely random user association. Recall from Section IV that our proposed utility function explicitly considers both the legitimate $UAV_i \longrightarrow \left\{U_{1,k}^{i}, U_{2,k}^{i}\right\}$ link and the estimated $UAV_i \longrightarrow \{e\}$ link during the user association process. Observe in Fig. 8 that this utility function results in better SEE performance than the other two methods that merely consider the legitimate link in their utility function. To elaborate, our method has the edge, because the SEE depends not only on the quality of the legitimate links, but also on the quality of the Eve's channel. Therefore, it is important to consider the quality of the eavesdropping channels in support of the user ordering decisions. Moreover, the poor performance of a random user ordering becomes explicit in Fig. 8, because it does not consider any information regarding the communication channels and blindly assigns SCs to users. The reduction

Benchmark	$s_k^{i,c}$	$s_{1,k}^{i,p}$	$s_{2,k}^{i,p}$
CRS	$\mathcal{W}_k^{i,c}$	$\mathcal{W}_{1,k}^{i,p}$	$\mathcal{W}_{2,k}^{i,p}$
C-NOMA	$\mathcal{W}_{2,k}^{i,p}$	$\mathcal{W}_{1,k}^{i,p}$	–
C-BF	–	$\mathcal{W}_{1,k}^{i,p}$	$\mathcal{W}_{2,k}^{i,p}$

TABLE IV
MAPPING OF MESSAGES TO STREAMS

of SEE becomes particularly pronounced for low values of K.

VII. CONCLUSIONS

In this article we proposed a secure and energy-efficient scheme for multi-carrier UAV-HetNets in which each UAV-cell relies on CRS for safeguarding the UAV's downlink transmissions against an Eve, whose channels are imperfectly known at the Tx. The system's performance was evaluated in terms of both its EE and secrecy. More explicitly, we maximized the SEE by jointly optimizing both the user association matrix and the RS-precoders as well as the time slot sharing and SC power allocation. Given the convexity of the resultant problem, it was decoupled into two convex sub-problems. More precisely, a new two-tier algorithm was proposed for finding ζ-optimal solutions by iterative block coordinate decent programming for the resultant intra-cell optimization problems. Moreover, user association was carried out by conceiving an efficient two-sided matching algorithm. Then, based on the intra-cell parameters obtained, the power of each SC used by the UAV cells was optimized. Finally, a user-swapping algorithm was designed for improving the user association results. Simulation results confirm the supremacy of CRS over the C-NOMA and the C-SDMA benchmarks.

APPENDIX A
PROOF OF THE OPTIMAL SEE FOR ICOP

Given that the ICOP sub-problem and the optimization problem proposed in Theorem 2 have identical conditions, one can infer that both problems have the same feasible set. In the first step, we define the arbitrary feasible solution set $\{\tilde{\mathbf{P}}_k^i, \tilde{\theta}, \tilde{p}_{k,R}^i, \tilde{p}_{k,J}^i\}$ of the original problem in (24), where $\{\tilde{\mathbf{P}}_k^{i^*}, \tilde{\theta}^*, \tilde{p}_{k,R}^{i*}, \tilde{p}_{k,J}^{i*}\}$ is the optimal solution of (24), seen in $A-1$ at the top of the next page. Upon invoking $(A-1)$ one can obtain $(A-2)$ and $(A-3)$ at the top of the next page. Invoking the definition of $f(\cdot)$ in (25) together with equations $(A-2)$ and $(A-3)$, we can deduce that the optimal value $f(\eta_{SEE}^*)$, which equals to zero, occurs at $\{\tilde{\mathbf{P}}_k^{i^*}, \tilde{\theta}^*, \tilde{p}_{k,R}^{i*}, \tilde{p}_{k,J}^{i*}\}$. Finally, we consider $\{\hat{\mathbf{P}}_k^i, \hat{\theta}, \hat{p}_{k,R}^i, \hat{p}_{k,J}^i\}$ as an arbitrary feasible solution of the transformed problem of (25) and $\{\hat{\mathbf{P}}_k^{i^*}, \hat{\theta}^*, \hat{p}_{k,R}^{i*}, \hat{p}_{k,J}^{i*}\}$ as the optimal solution of (25), respectively. We also consider the fact that $f(\eta_{SEE}^*) = 0$. Therefore, one can rewrite $(A-3)$ as $(A-4)$ at the top of the next page.

Using some straightforward manipulations, we arrive $(A-5)$ at the top of the next page. By invoking $(A-5)$, one can readily infer that $\{\hat{\mathbf{P}}_k^{i^*}, \hat{\theta}^*, \hat{p}_{k,R}^{i*}, \hat{p}_{k,J}^{i*}\}$ is an optimal solution for the original problem of (24). Finally, based on $(A-2)$ and $(A-3)$, $\{\tilde{\mathbf{P}}_k^{i^*}, \tilde{\theta}^*, \tilde{p}_{k,R}^{i*}, \tilde{p}_{k,J}^{i*}\}$ equals $\{\hat{\mathbf{P}}_k^{i^*}, \hat{\theta}^*, \hat{p}_{k,R}^{i*}, \hat{p}_{k,J}^{i*}\}$ iff $f(\eta_{SEE}^*) = 0$.

The inequality constraints appearing originate from the fact that the original active counterparts are non-convex owing to having non-affine functions at both sides of $(26-C_1 : C_4)$. So, to tackle the non-convexity and maintain the generality of the problem, the inequality constraints have to be specifically defined for ensuring that they would be active at the optimum.

APPENDIX B
PROOF OF THE CONSTRAINT (31-C_1)

Following the principle of the SPCA, $f_{k,0}^i$ can respectively represent the lower-bound of $C_k^{i,c}$. Increasing the lower-bound values and simultaneously reducing the upper-bounds will boost the left-side of the constraints, which is needed here, so that the constraint (26-C_1) would be active at the optimum. Despite this linearization, it can be seen by invoking the definitions of $C_k^{i,c}$ that the constraints (26-C_1) is still non-convex. In what follows we elaborate the procedure of convexifying of (26-C_1). To handle the non-convexity of these constraints we construct a suitable inner convex subset for approximating the non-convex feasible solution set. Along these lines, by substituting the definition of $C_k^{i,c}$ at (26-C_1) we have $C_1 : \ f_{k,0}^i \leq \min\left\{C_{1,k}^{i,c^{(1)}}, C_{2,k}^{i,c^{(1)}} + C_{2,k}^{i,c^{(2)}}\right\}$. Then we can approximate it by its linear Taylor expansion as follows:

$$\Theta^{[t]}\left(\theta, \beta_{c,1}^{(1)}\right) \geq f_{k,0}^i, \qquad (B-1)$$

$$\Theta^{[t]}\left(\theta, \beta_{c,2}^{(1)}\right) + \Theta^{[t]}\left(1-\theta, \beta_{c,2}^{(2)}\right) \geq f_{k,0}^i, \qquad (B-2)$$

where we have defined $\Theta^{[m]}(x,y) \triangleq \frac{1}{2}(x^{[m]} + y^{[m]})(x+y) - \frac{1}{4}(x^{[m]} + y^{[m]})^2 - \frac{1}{4}(x-y)^2$, and $\bar{\Theta}^{[m]}(x,y) \triangleq \frac{1}{4}(x+y)^2 + \frac{1}{4}(x^{[m]} - y^{[m]})^2 - \frac{1}{2}(x^{[m]} - y^{[m]})(x-y)$ for the linear approximation of the terms, which are the product of two variables. With the aim of the linearization of (26-C_1), after substituting the definition of $C_{1,k}^{i,c^{(1)}}, C_{2,k}^{i,c^{(1)}}$ and $C_{2,k}^{i,c^{(2)}}$ and using some variable transformations, the three extra auxiliary constraints are formulated for $\forall j \in \{1,2\}$, as follows:

$$1 + \rho_{c,1}^{(1)} - 2^{\beta_{c,1}^{(1)}} \geq 0, \qquad (B-3)$$

$$1 + \rho_{c,2}^{(j)} - 2^{\beta_{c,2}^{(j)}} \geq 0, \qquad (B-4)$$

$$\gamma_{n,k}^{i,\mathrm{c}\ (1)} \geq \rho_{c,n}^{(1)}, \qquad (B-5)$$

$$\gamma_{2,k}^{i,\mathrm{c}\ (2)} \geq \rho_{c,2}^{(j)}. \qquad (B-6)$$

Although $(B-3)$ and $(B-4)$ is convex, upon substituting the definition of $\gamma_{n,k}^{i,\mathrm{c}\ (1)}$ and $\gamma_{2,k}^{i,\mathrm{c}\ (2)}$ into $(B-5)$ and $(B-6)$, it can be represented as the difference of two convex functions (DC decomposition) and thus it is non-convex. To deal with this non-convexity, we first write the equivalent DC decomposition of $(B-5)$ as:

$$\left|\left(\mathbf{h}_{n,k}^i\right)^H \mathbf{p}_{1,k}^{i,p}\right| + \left|\left(\mathbf{h}_{n,k}^i\right)^H \mathbf{p}_{2,k}^{i,p}\right|^2 - \frac{\left|\left(\mathbf{h}_{n,k}^i\right)^H \mathbf{p}_k^{i,c}\right|^2}{\rho_{c,n}^{(1)}} \leq 0, \ (B-7)$$

To deal with $(B-7)$, we relax the concave parts of the DC constraints with the aid of their first-order Taylor expansions. Then , $(B-7)$ is approximated around the point $\left(\mathbf{p}_k^{i,c\ [t]}, \rho_{c,n}^{(1)\ [t]}\right)$ at the t-th iteration by:

$$\left|\left(\mathbf{h}_{n,k}^i\right)^H \mathbf{p}_{1,k}^{i,p}\right|^2 + \left|\left(\mathbf{h}_{n,k}^i\right)^H \mathbf{p}_{2,k}^{i,p}\right|^2 + \delta^2 P_k^M \left\|\mathbf{c}_{n,k}^i\right\|^2 \ (B-8)$$
$$-\Psi^{[t]}\left(\mathbf{p}_k^{i,c}, \rho_{c,n}^{(1)}; \mathbf{h}_{n,k}^i\right) \leq 0,$$

$$\eta^*_{SEE^i_k}=\frac{\sum_{n=0}^{N_k}\left(f^i_{k,n}(\tilde{\mathbf{P}}^{i^*}_k,\tilde{\theta}^*,\tilde{p}^{i*}_{k,R},\tilde{p}^{i*}_{k,J})-g^i_{k,n}(\tilde{\mathbf{P}}^{i^*}_k,\tilde{\theta}^*,\tilde{p}^{i*}_{k,R},\tilde{p}^{i*}_{k,J})\right)}{P_m+||\tilde{\mathbf{p}}^{i,c^*}_k||^2+\sum_{n=1}^{N_k}||\tilde{\mathbf{p}}^{i,p^*}_{n,k}||^2}\geq\frac{\sum_{n=0}^{N_k}\left(f^i_{k,n}(\tilde{\mathbf{P}}^{i}_k,\tilde{\theta},\tilde{p}^{i}_{k,R},\tilde{p}^{i}_{k,J})-g^i_{k,n}(\tilde{\mathbf{P}}^{i}_k,\tilde{\theta},\tilde{p}^{i}_{k,R},\tilde{p}^{i}_{k,J})\right)}{P_m+||\tilde{\mathbf{p}}^{i,c}_k||^2+\sum_{n=1}^{N_k}||\tilde{\mathbf{p}}^{i,p}_{n,k}||^2},$$

$$(A-1)$$

$$\sum_{n=0}^{N_k}\left(f^i_{k,n}\left(\tilde{\mathbf{P}}^{i^*}_k,\tilde{\theta}^*,\tilde{p}^{i*}_{k,R},\tilde{p}^{i*}_{k,J}\right)-g^i_{k,n}\left(\tilde{\mathbf{P}}^{i^*}_k,\tilde{\theta}^*,\tilde{p}^{i*}_{k,R},\tilde{p}^{i*}_{k,J}\right)\right)-\eta^*_{SEE}\left(P_m+||\tilde{\mathbf{p}}^{i,c^*}_k||^2+\sum_{n=1}^{N_k}||\tilde{\mathbf{p}}^{i,p^*}_{n,k}||^2\right)=0,\ (A-2)$$

$$\sum_{n=0}^{N_k}\left(f^i_{k,n}\left(\tilde{\mathbf{P}}^{i}_k,\tilde{\theta},\tilde{p}^{i}_{k,R},\tilde{p}^{i}_{k,J}\right)-g^i_{k,n}\left(\tilde{\mathbf{P}}^{i}_k,\tilde{\theta},\tilde{p}^{i}_{k,R},\tilde{p}^{i}_{k,J}\right)\right)-\eta^*_{SEE}\left(P_m+||\tilde{\mathbf{p}}^{i,c}_k||^2+\sum_{n=1}^{N_k}||\tilde{\mathbf{p}}^{i,p}_{n,k}||^2\right)\leq 0,\ (A-3)$$

$$f\left(\eta^*_{SEE}\right)=\sum_{n=0}^{N_k}\left(f^i_{k,n}\left(\hat{\mathbf{P}}^{i^*}_k,\hat{\theta}^*,\hat{p}^{i*}_{k,R},\hat{p}^{i*}_{k,J}\right)-g^i_{k,n}\left(\hat{\mathbf{P}}^{i^*}_k,\hat{\theta}^*,\hat{p}^{i*}_{k,R},\hat{p}^{i*}_{k,J}\right)-\eta^*_{SEE}\left(P_m+||\hat{\mathbf{p}}^{i,c^*}_k||^2+\sum_{n=1}^{N_k}||\hat{\mathbf{p}}^{i,p^*}_{n,k}||^2\right)\right.$$

$$0\geq\sum_{n=0}^{N_k}\left(f^i_{k,n}\left(\hat{\mathbf{P}}^{i}_k,\hat{\theta},\hat{p}^{i}_{k,R},\hat{p}^{i}_{k,J}\right)-g^i_{k,n}\left(\hat{\mathbf{P}}^{i}_k,\hat{\theta},\hat{p}^{i}_{k,R},\hat{p}^{i}_{k,J}\right)\right)-\eta^*_{SEE}\left(P_m+||\hat{\mathbf{p}}^{i,c}_k||^2+\sum_{n=1}^{N_k}||\hat{\mathbf{p}}^{i,p}_{n,k}||^2\right),\ (A-4)$$

$$\frac{\sum_{n=0}^{N_k}\left(f^i_{k,n}\left(\hat{\mathbf{P}}^{i}_k,\hat{\theta},\hat{p}^{i}_{k,R},\hat{p}^{i}_{k,J}\right)-g^i_{k,n}\left(\hat{\mathbf{P}}^{i}_k,\hat{\theta},\hat{p}^{i}_{k,R},\hat{p}^{i}_{k,J}\right)\right)}{P_m+||\hat{\mathbf{p}}^{i,c}_k||^2+\sum_{n=1}^{N_k}||\hat{\mathbf{p}}^{i,p}_{n,k}||^2}\leq\frac{\sum_{n=0}^{N_k}\left(f^i_{k,n}\left(\hat{\mathbf{P}}^{i^*}_k,\hat{\theta}^*,\hat{p}^{i*}_{k,R},\hat{p}^{i*}_{k,J}\right)-g^i_{k,n}\left(\hat{\mathbf{P}}^{i^*}_k,\hat{\theta}^*,\hat{p}^{i*}_{k,R},\hat{p}^{i*}_{k,J}\right)\right)}{P_m+||\hat{\mathbf{p}}^{i,c^*}_k||^2+\sum_{n=1}^{N_k}||\hat{\mathbf{p}}^{i,p^*}_{n,k}||^2}$$
$$=\eta^*_{SEE},\qquad(A-5)$$

where we have $\Psi^{[t]}\left(\mathbf{u},x;\,\mathbf{h}\right)\triangleq\frac{2\Re e\left\{\left(\mathbf{u}^{[t]}\right)^H\mathbf{h}\mathbf{h}^H\mathbf{u}\right\}}{x^{[t]}}-\frac{\left|\mathbf{h}^H\mathbf{u}^{[t]}\right|^2x}{\left(x^{[t]}\right)^2}$. Upon using the same approach, we rewrite $(B-6)$ as:

$$p^i_{k,J}\left|\left(\mathbf{h}^i_{2,k}\right)^H\hat{\mathbf{p}}^i_{k,z}\right|^2+P^M_k\left\|\mathbf{c}^i_{2,k}\right\|^2-\Psi^{[t]}\left(\delta^i_{k,R},\rho^{(2)}_{c,2};\,f^i_{1,2,k}\right)+\delta^2\leq 0,\quad(B-9)$$

Appendix C
Proof of the constraint (31-C_3)

The constraint (31-C_3) can be equivalently rewritten as follows:

$$g^i_{k,0}\geq\max_{\Lambda^i_{e,k}}C^{i,c}_{e,k}\qquad(C-1)$$

Problem $(C-1)$ represents search over the possible values of CSI uncertainties to find the worst-case. On the other hand, based on what we inferred earlier from (29-C_3) and (29-C_8), the goal is to minimize $C^{i,c}_{e,k}$ by minimizing its ceiling rate $\alpha_{c,e}$. Incorporating this into $(C-1)$, it is expected that this ceiling does not exceed the predefined target rate $r^{i,c}_k$, i.e. $C^{i,c}_{e,k}\leq\alpha_{c,e}\leq r^{i,c}_k$ for various imperfections. Given this fact, $(C-1)$ is transformed into some extra artificial constraints, constraints, with the objective of linearization. Thus, by inserting the definition of $C^{i,c}_{e,k}$ as well as as by exploiting the auxiliary variables introduced in (31) for $\hat{\gamma}^{i,c\,(1)}_{e,k}$, $\hat{\gamma}^{i,c\,(2)}_{e,k}$ along with new auxiliary variables, the problem $(C-1)$ after some trivial manipulation can be recast as:

$$\theta\log_2\left(1+\rho^{(1)}_{c,e}\right)+(1-\theta)\log_2\left(1+\rho^{(2)}_{c,e}\right)\leq\alpha_{c,e},\quad(C-2)$$

$$\frac{x^2_{c,e}}{\sum_{n=1}^{2}u_{n,c,e}+p_{M,k}\left\|\mathbf{c}^i_{e,k}\right\|^2+\delta^2}\leq\rho^{(1)}_{c,e},\qquad(C-3)$$

$$\frac{y^2_{c,e}}{v_{c,e}+p_{M,k}\left\|\mathbf{c}^i_{e,k}\right\|^2+\delta^2}\leq\rho^{(2)}_{c,e},\qquad(C-4)$$

$$\max_{\mathbf{\Delta n}_{\mathbf{h}^i_{e,k}}}\left|\mathbf{h}^i_{e,k}{}^H\mathbf{p}^{i,c}_k\right|\leq x_{c,e},\qquad(C-5)$$

$$\min_{\mathbf{\Delta n}_{\mathbf{h}^i_{e,k}}}\left|\mathbf{h}^i_{e,k}{}^H\mathbf{p}^{i,p}_{n,k}\right|^2\geq u_{n,c,e},\ n\in\{1,2\},\qquad(C-6)$$

$$\max_{\triangle f^i_{e,k}}\delta^i_{k,R}\left|f^i_{e,k}\right|\leq y_{c,e},\qquad(C-7)$$

$$\min_{\mathbf{\Delta n}_{\mathbf{h}^i_{e,k}}}\ p^i_{k,j}\left|\mathbf{h}^i_{e,k}{}^H\mathbf{p}_z\right|^2\geq v_{c,e}.\qquad(C-8)$$

However, $(C(2:8))$ are still non-convex. To handle the non-convexity of these constraints we construct a suitable inner convex subset for approximating the non-convex feasible solution set. To this effect, we first approximate $(C-2)$ by its linear Taylor expansion to obtain $\bar{\Theta}^{[t]}\left(\theta,\beta^{(1)}_{c,e}\right)+\bar{\Theta}^{[t]}\left(1-\theta,\beta^{(2)}_{c,e}\right)\leq\alpha_{c,e}$, where we have defined $\Theta^{[t]}\left(x,y\right)$ and $\bar{\Theta}^{[m]}\left(x,y\right)$ in (31) for the linear approximation of the terms, which are the product of two variables. To circumvent the non-convexity of $(C-3)$, three extra artificial constraints (31-C_3 (III)), (31-C_3(IV)) and (31-C_3(VII)) are introduced. Similarly, as for $(C-4)$, we have equivalently derived (31-C_3 (V)) and (31-C_3(VI)).

To handle the non-convex constraints $(C-(5:8))$, we exploit the following proposition.

Proposition 3. *For the terms* $\mathcal{D}_1\left(\mathbf{\Delta h}\right)\triangleq\left|\left(\hat{\mathbf{h}}+\mathbf{\Delta h}\right)^H\mathbf{u}\right|$ *and* $\mathcal{D}_2\left(\mathbf{\Delta h}\right)\triangleq\left|\left(\hat{\mathbf{h}}+\mathbf{\Delta h}\right)^H\mathbf{u}\right|^2$ *with norm-bounded variable* $\left\|\mathbf{\Delta h}\right\|_2\leq\sigma$*, the following minimizer and maximizer can be presented:*

$$\min_{\|\mathbf{\Delta h}\|_2 \leq \sigma} \mathcal{D}_1\left(\mathbf{\Delta h}\right) = \left|\hat{\mathbf{h}}^H \mathbf{u}\right| + \sigma \left\|\mathbf{u}\right\|_2, \qquad (C-9)$$

$$\min_{\|\mathbf{\Delta h}\|_2 \leq \sigma} \mathcal{D}_2\left(\mathbf{\Delta h}\right) = Tr\left[\left(\hat{\mathbf{H}} - \mu \mathbf{I}\right)\mathbf{U}\right], \qquad (C-10)$$

$$\max_{\|\mathbf{\Delta h}\|_2 \leq \sigma} \mathcal{D}_2\left(\mathbf{\Delta h}\right) = Tr\left[\left(\hat{\mathbf{H}} + \mu \mathbf{I}\right)\mathbf{U}\right], \qquad (C-11)$$

where $\hat{\mathbf{H}} \triangleq \hat{\mathbf{h}}\hat{\mathbf{h}}^H$, $\mathbf{U} \triangleq \mathbf{u}\mathbf{u}^H$, $\mu \triangleq \sigma^2 + 2\sigma \left\|\hat{\mathbf{h}}\right\|_2$.

Proof:
Please refer to [40]. ■

Using proposition 3, we can relax the right-side of $(C-(5:8))$, leading to respectively as presented in (31-C_3(VI))-(31-C_3(X)).

REFERENCES

[1] F. Tariq, M. R. A. Khandaker, K. -K. Wong, M. A. Imran, M. Bennis and M. Debbah, "A Speculative Study on 6G," *in IEEE Wireless Communications*, vol. 27, no. 4, pp. 118-125, August 2020.

[2] Z. Wei, L. Yang, D. W. K. Ng, J. Yuan and L. Hanzo, "On the Performance Gain of NOMA Over OMA in Uplink Communication Systems," *in IEEE Transactions on Communications*, vol. 68, no. 1, pp. 536-568, Jan. 2020.

[3] Y. Zou, J. Zhu, X. Wang, and L. Hanzo. "A survey on wireless security: Technical challenges, recent advances, and future trends." *Proceedings of the IEEE 104*, no. 9 (2016): 1727-1765.

[4] Z. Kong, S. Yang, D. Wang and L. Hanzo, "Robust Beamforming and Jamming for Enhancing the Physical Layer Security of Full Duplex Radios," *in IEEE Transactions on Information Forensics and Security*, vol. 14, no. 12, pp. 3151-3159, Dec. 2019, doi: 10.1109/TIFS.2019.2908481.

[5] Z. Kong, S. Yang, F. Wu, S. Peng, L. Zhong and L. Hanzo, "Iterative Distributed Minimum Total MSE Approach for Secure Communications in MIMO Interference Channels," *in IEEE Transactions on Information Forensics and Security*, vol. 11, no. 3, pp. 594-608, March 2016, doi: 10.1109/TIFS.2015.2493888.

[6] M. Moradikia, H. Bastami, A. Kuhestani, H. Behroozi and L. Hanzo, "Cooperative Secure Transmission Relying on Optimal Power Allocation in the Presence of Untrusted Relays, A Passive Eavesdropper and Hardware Impairments," *in IEEE Access*, vol. 7, pp. 116942-116964, 2019.

[7] H. Bastami, M. Moradikia, H. Behroozi, RC. de Lamare, A. Abdelhadi, and Z. Ding. "Secrecy Rate Maximization for Hardware Impaired Untrusted Relaying Network with Deep Learning." *arXiv preprint arXiv:2101.02749 (2021).*

[8] S. Mashdour, M. Moradikia, and P. Yeoh. "Secure mm-Wave communications with imperfect hardware and uncertain eavesdropper location." *Transactions on Emerging Telecommunications Technologies 31*, no. 10 (2020): e4016.

[9] H. Bastami, M. Moradikia, M. Letafati, A. Abdelhadi and H. Behroozi, "Outage-Constrained Robust and Secure Design for Downlink Rate-Splitting UAV Networks," *2021 IEEE International Conference on Communications Workshops (ICC Workshops), 2021*, pp. 1-7, doi: 10.1109/ICCWorkshops50388.2021.9473675.

[10] K. Xu, M. -M. Zhao, Y. Cai and L. Hanzo, "Low-Complexity Joint Power Allocation and Trajectory Design for UAV-Enabled Secure Communications With Power Splitting," *in IEEE Transactions on Communications*, vol. 69, no. 3, pp. 1896-1911, March 2021, doi: 10.1109/TCOMM.2020.3042462.

[11] S. A. Hoseini, F. Bouhafs and F. den Hartog, "A Practical Implementation of Physical Layer Security in Wireless Networks," 2022 IEEE 19th Annual Consumer Communications & Networking Conference (CCNC), 2022, pp. 1-4, doi: 10.1109/CCNC49033.2022.9700672.

[12] K. Ryland, "Software-Defined Radio Implementation of Two Physical Layer Security Techniques," *Virginia Tech*, 2018.

[13] R. Negi and S. Goel, "Secret communication using artificial noise," *in IEEE Vehicular Technology Conference,* 2005, vol. 62, no. 3, p. 1906.

[14] A. Al-Hourani, S. Kandeepan and S. Lardner, "Optimal LAP Altitude for Maximum Coverage," *in IEEE Wireless Communications Letters*, vol. 3, no. 6, pp. 569-572, Dec. 2014, doi: 10.1109/LWC.2014.2342736.

[15] L. Xiao, Y. Xu, D. Yang and Y. Zeng, "Secrecy Energy Efficiency Maximization for UAV-Enabled Mobile Relaying," *in IEEE Transactions on Green Communications and Networking*, vol. 4, no. 1, pp. 180-193, March 2020.

[16] J. Ouyang, M. Lin, Y. Zou, W. Zhu and D. Massicotte, "Secrecy Energy Efficiency Maximization in Cognitive Radio Networks," *in IEEE Access*, vol. 5, pp. 2641-2650, 2017.

[17] Y. Jiang, Y. Zou, J. Ouyang and J. Zhu, "Secrecy Energy Efficiency Optimization for Artificial Noise Aided Physical-Layer Security in OFDM-Based Cognitive Radio Networks," *in IEEE Transactions on Vehicular Technology*, vol. 67, no. 12, pp. 11858-11872, Dec. 2018.

[18] H. Fu, S. Feng, W. Tang and D. W. K. Ng, "Robust Secure Beamforming Design for Two-User Downlink MISO Rate-Splitting Systems," *in IEEE Transactions on Wireless Communications,* vol. 19, no. 12, pp. 8351-8365, Dec. 2020.

[19] Y. Sun, D. W. K. Ng, J. Zhu and R. Schober, "Robust and Secure Resource Allocation for Full-Duplex MISO Multicarrier NOMA Systems," *in IEEE Transactions on Communications*, vol. 66, no. 9, pp. 4119-4137, Sept. 2018.

[20] H. Zhang, J. Zhang and K. Long, "Energy Efficiency Optimization for NOMA UAV Network With Imperfect CSI," *in IEEE Journal on Selected Areas in Communications*, vol. 38, no. 12, pp. 2798-2809, Dec. 2020.

[21] Y. Liu, Y. Yang, L. -L. Yang and L. Hanzo, "Physical Layer Security of Spatially Modulated Sparse-Code Multiple Access in Aeronautical Ad-hoc Networking," *in IEEE Transactions on Vehicular Technology*, vol. 70, no. 3, pp. 2436-2447, March 2021.

[22] F. Shu, X. Wu, J. Li, R. Chen, and B. Vucetic. "Robust synthesis scheme for secure multi-beam directional modulation in broadcasting systems." *IEEE Access* 4 (2016): 6614-6623.

[23] S. Ahmed, M. Z. Chowdhury, S. R. Sabuj, M. I. Alam and Y. M. Jang, "Energy-Efficient UAV Relaying Robust Resource Allocation in Uncertain Adversarial Networks," in IEEE Access, vol. 9, pp. 59920-59934, 2021.

[24] W. Jaafar, S. Naser, S. Muhaidat, P. C. Sofotasios and H. Yanikomeroglu, "On the Downlink Performance of RSMA-Based UAV Communications," *in IEEE Transactions on Vehicular Technology*, vol. 69, no. 12, pp. 16258-16263, Dec. 2020.

[25] Y. Mao, B. Clerckx and V. O. K. Li, "Energy Efficiency of Rate-Splitting Multiple Access, and Performance Benefits over SDMA and NOMA," *2018 15th International Symposium on Wireless Communication Systems (ISWCS), 2018*, pp. 1-5.

[26] J. Zhang, B. Clerckx, J. Ge and Y. Mao, "Cooperative rate splitting for MISO broadcast channel with user relaying, and performance benefits over cooperative NOMA," *in IEEE Signal Processing Letters*, vol. 26, no. 11, pp. 1678-1682, Nov 2019.

[27] W. Khawaja, I. Guvenc and D. Matolak, "UWB Channel Sounding and Modeling for UAV Air-to-Ground Propagation Channels," *in Proc. IEEE Global Commun. Conf. (GLOBECOM'16)*, Washington, USA, Dec. 2016, pp. 1-7.

[28] A. A. Khuwaja, Y. Chen, N. Zhao, M. -S. Alouini and P. Dobbins, "A Survey of Channel Modeling for UAV Communications," *in IEEE Communications Surveys & Tutorials*, vol. 20, no. 4, pp. 2804-2821, Fourth quarter 2018, doi: 10.1109/COMST.2018.2856587

[29] Y. Mao, B. Clerckx and V. O. K. Li, "Rate-splitting for multi-antenna non-orthogonal unicast and multicast transmission: Spectral and energy efficiency analysis," *in IEEE Transactions on Communications*, vol. 67, no. 12, pp. 8754-8770, Dec. 2019.

[30] G. Zhou, Y. Mao, and B. Clerckx, "Rate-splitting multiple access for multi-antenna downlink communication systems: spectral and energy efficiency tradeoff," *arXiv preprint:2001.03206, 2020.*

[31] B. Clerckx, Y. Mao, R. Schober and H. V. Poor, "Rate-splitting unifying SDMA, OMA, NOMA, and multicasting in MISO broadcast channel: A simple two-user rate analysis," *in IEEE Wireless Communications Letters*, vol. 9, no. 3, pp. 349-353, March 2020.

[32] B. Clerckx, H. Joudeh, C. Hao, M. Dai, and B. Rassouli, "Rate splitting for MIMO wireless networks: a promising PHY-layer strategy for LTE evolution," *in IEEE Communications Magazine*, vol. 54, no. 5, pp. 98-105, May 2016.

[33] Y. Mao, B. Clerckx, J. Zhang, V.O.K. Li, and M. Arafah, "Max-min Fairness of K-user Cooperative Rate-Splitting in MISO Broadcast Channel with User Relaying" *IEEE Trans. on Wireless Comm.,* col. 19, no. 10, pp. 6362-6376, Oct. 2020.

[34] P. Li, M. Chen, Y. Mao, Z. Yang, B. Clerckx and M. Shikh-Bahaei, "Cooperative Rate-Splitting for Secrecy Sum-Rate Enhancement in Multi-antenna Broadcast Channels," *2020 IEEE 31st Annual International Symposium on Personal, Indoor and Mobile Radio Communications, 2020*, pp. 1-6.

[35] H. Joudeh and B. Clerckx, “Sum-Rate Maximization for Linearly Precoded Downlink Multiuser MISO Systems with Partial CSIT: A Rate-Splitting Approach,” *IEEE Trans. on Comm.* vol. 64, no. 11, pp. 4847-4861, Nov 2016.

[36] T. Bai, J. Wang, Y. Ren and L. Hanzo, "Energy-Efficient Computation Offloading for Secure UAV-Edge-Computing Systems," *in IEEE Transactions on Vehicular Technology*, vol. 68, no. 6, pp. 6074-6087, June 2019, doi: 10.1109/TVT.2019.2912227.

[37] X. Chu, H. Zhang, W. Huangfu, W. Liu, Y. Ren, J. Dong, and K. Long, "Subchannel Assignment and Power Optimization for Energy-Efficient NOMA Heterogeneous Network," *2019 IEEE Global Communications Conference (GLOBECOM), 2019*, pp. 1-6, doi: 10.1109/GLOBECOM38437.2019.9014308.

[38] H. Zhang, N. Yang, K. Long, M. Pan, G. K. Karagiannidis and A. Nallanathan, "Energy Efficient Resource Allocation for Secure NOMA Networks," *2018 IEEE 87th Vehicular Technology Conference (VTC Spring), 2018*, pp. 1-6, doi: 10.1109/VTCSpring.2018.8417649.

[39] L. Meng, Q. Wang, Z. Ji, M. Nie, B. Ji, C. Li and K. Song, "Resource allocation on secrecy energy efficiency for C-RAN with artificial noise," *Wireless Network 26*, 639–650 (2020). https://doi.org/10.1007/s11276-019-02160-x.

[40] E. A. Gharavol, Y. Liang and K. Mouthaan, "Robust Downlink Beamforming in Multiuser MISO Cognitive Radio Networks With Imperfect Channel-State Information," *in IEEE Transactions on Vehicular Technology*, vol. 59, no. 6, pp. 2852-2860, July 2010.

[41] S. Boyd and L. Vanderberghe, “Convex Optimization,” *Cambridge, U.K.: Cambridge Univ. Press*, 2004.